Characterization of SOC1's Central Role in Flowering by the Identification of Its Upstream and Downstream Regulators[1][C][W]

Richard G.H. Immink[2]*, David Posé[2], Silvia Ferrario, Felix Ott, Kerstin Kaufmann, Felipe Leal Valentim, Stefan de Folter[3], Froukje van der Wal, Aalt D.J. van Dijk, Markus Schmid, and Gerco C. Angenent

Plant Research International, Bioscience, 6708 PB Wageningen, The Netherlands (R.G.H.I., S.F., K.K., F.L.V., S.d.F., F.v.d.W., A.D.J.v.D., G.C.A.); Consortium for Improved Plant Yield, 6700 AB Wageningen, The Netherlands (R.G.H.I., G.C.A.); Department of Molecular Biology, Max Planck Institute for Developmental Biology, 72076 Tuebingen, Germany (D.P., F.O., M.S.); and Laboratory of Molecular Biology, Wageningen University, 6708 PB Wageningen, The Netherlands (K.K., G.C.A.)

The transition from vegetative to reproductive development is one of the most important phase changes in the plant life cycle. This step is controlled by various environmental signals that are integrated at the molecular level by so-called floral integrators. One such floral integrator in Arabidopsis (*Arabidopsis thaliana*) is the MADS domain transcription factor SUPPRESSOR OF OVEREXPRESSION OF CONSTANS1 (SOC1). Despite extensive genetic studies, little is known about the transcriptional control of *SOC1*, and we are just starting to explore the network of genes under the direct control of SOC1 transcription factor complexes. Here, we show that several MADS domain proteins, including SOC1 heterodimers, are able to bind *SOC1* regulatory sequences. Genome-wide target gene analysis by ChIP-seq confirmed the binding of SOC1 to its own locus and shows that it also binds to a plethora of flowering-time regulatory and floral homeotic genes. In turn, the encoded floral homeotic MADS domain proteins appear to bind *SOC1* regulatory sequences. Subsequent in planta analyses revealed *SOC1* repression by several floral homeotic MADS domain proteins, and we show that, mechanistically, this depends on the presence of the SOC1 protein. Together, our data show that SOC1 constitutes a major hub in the regulatory networks underlying floral timing and flower development and that these networks are composed of many positive and negative autoregulatory and feedback loops. The latter seems to be crucial for the generation of a robust flower-inducing signal, followed shortly after by repression of the *SOC1* floral integrator.

Plants have an impressive capacity to adapt to changing environmental conditions. An important characteristic is their ability to control flowering time and to flower under the most optimal conditions (Franks et al., 2007; Izawa, 2007). Plants sense their environment continuously and act on signals such as light quality, daylength, temperature, and the availability of nutrients. The individual environmental signals are integrated with the endogenous flowering program, which ultimately gives rise to a flower-inducing stimulus (Parcy, 2005; Turck et al., 2008). Various members of the MADS box transcription factor (TF) family play essential roles in the molecular signaling cascades underlying the environmental sensing and function either as activators or repressors of the flowering process (for review, see Michaels, 2009; Yant et al., 2009; Kaufmann et al., 2010a). In the model species Arabidopsis (*Arabidopsis thaliana*), the *FLOWERING LOCUS T* (*FT*), *LEAFY* (*LFY*), and *SUPPRESSOR OF OVEREXPRESSION OF CONSTANS1* (*SOC1*) genes act as central floral integrators (Blazquez et al., 1998; Nilsson et al., 1998; Samach et al., 2000). Of these, the FT protein appears to be the flowering stimulus that moves from leaves into the shoot apical meristem region, where it evokes the transition from vegetative to reproductive meristem identity (Corbesier et al., 2007; Mathieu et al., 2007).

The *SOC1* floral integrator is a member of the MADS box TF family, and its expression is regulated by the daylength and vernalization pathways (Hepworth et al., 2002). *SOC1* expression is up-regulated under long-day

[1] This work was supported by the European Molecular Biology Organization (grant to S.F.), the European Research Area in Plant Genomics BLOOMNET project (grant no. SCHM1560/7–1 to D.P., M.S., R.G.H.I., K.K., and G.C.A.), and the Centre for Biosystems Genomics in The Netherlands.

[2] These authors contributed equally to the article.

[3] Present address: Laboratorio Nacional de Genómica para la Biodiversidad, Centro de Investigación y de Estudios Avanzados del Instituto Politécnico Nacional, CP 36821 Irapuato, Guanajuato, Mexico.

* Corresponding author; e-mail richard.immink@wur.nl.

The author responsible for distribution of materials integral to the findings presented in this article in accordance with the policy described in the Instructions for Authors (www.plantphysiol.org) is: Richard G.H. Immink (richard.immink@wur.nl).

[C] Some figures in this article are displayed in color online but in black and white in the print edition.

[W] The online version of this article contains Web-only data.

www.plantphysiol.org/cgi/doi/10.1104/pp.112.202614

(LD) conditions by CONSTANS, in a process that to a large extent depends on the presence of the FT protein (Samach et al., 2000; Yoo et al., 2005). Furthermore, *SOC1* integrates the GA-mediated flowering-time signal with these environmental cues (Moon et al., 2003). A recent genetic study showed that the Arabidopsis *SOC1* clade members *AGAMOUS-LIKE42* (*AGL42*), *AGL71*, and *AGL72* also contribute to the GA-mediated transition to flowering; however, *SOC1* appears to be the major player in this response (Dorca-Fornell et al., 2011). FLOWERING LOCUS C (FLC) is the central player in the vernalization pathway, and this MADS domain TF represses the expression of *SOC1* via direct binding to the *SOC1* promoter region (Hepworth et al., 2002; Deng et al., 2011). FLC interacts with the MADS domain protein SHORT VEGETATIVE PHASE (SVP), which also acts as a floral repressor and binds *SOC1* regulatory sequences as well (Hartmann et al., 2000; Li et al., 2008; Tao et al., 2012). These floral repressors are counteracted by AGL24, which acts as a direct inducer of *SOC1* and flowering (Michaels et al., 2003). In addition, *SOC1* is controlled by an age-dependent mechanism involving *SQUAMOSA-BINDING FACTOR-LIKE9* and *microRNA156* (*miR156*; Wang et al., 2009). Besides this transcriptional control, *SOC1* mRNA levels appear to be posttranscriptionally regulated by the RNA-binding protein EARLY FLOWERING9 (ELF9), which supposedly targets *SOC1* transcripts for nonsense-mediated mRNA decay (Song et al., 2009). Recently, it was shown that SOC1 activity is also regulated at the protein level by a PIN1-type parvulin, which is involved in cis/trans-isomerization of phosphorylated Ser/Thr-Pro motifs (Wang et al., 2010). Jointly, these complex regulatory mechanisms ensure that *SOC1* reaches its threshold value for triggering the floral transition at the right moment during plant development and under environmental conditions that are favorable for reproduction.

Because of the important and central role of SOC1 in the integration of flowering-time signals, it is of high interest to identify the genes under its direct control. A small set of genes that act downstream of SOC1 are known from a microarray experiment (Seo et al., 2009), and recently, a genome-wide analysis reported target genes based on a ChIP-chip experiment using a SOC1 overexpression line (Tao et al., 2012). Furthermore, a peak of *SOC1* expression in the shoot apical meristem (SAM) just prior to the floral transition precedes *LFY* up-regulation, which could be explained by direct binding of SOC1 to *LFY* regulatory sequences (Lee et al., 2008), although *LFY* was not identified as a direct SOC1 target in the study by Tao et al. (2012). In turn, LFY is involved in the activation of the floral meristem identity gene *APETALA1* (*AP1*), resulting in flower meristem initiation (Liljegren et al., 1999; Benlloch et al., 2011; Moyroud et al., 2011; Pastore et al., 2011; Winter et al., 2011). *SOC1* is expressed initially within the emerging flower meristems, but this signal disappears in stage 1 and 2 flowers (Borner et al., 2000; Samach et al., 2000). *SOC1* expression in the floral meristem is proposed to prevent the precocious expression of B- and C-class floral organ identity genes via SEPALLATA3 (SEP3) and, hence, the maintenance of meristematic activity (Liu et al., 2009). In parallel, SOC1 may repress the B-type genes by direct binding to their regulatory sequences (Gregis et al., 2009). Shortly after the emergence of the floral meristem, *SOC1* gets repressed in the floral meristem due to increased AP1 levels (Liu et al., 2007). This transient repression of *SOC1* during the early stages of flower meristem development is essential because ectopic expression of *SOC1* affects further floral development severely (Borner et al., 2000; Liu et al., 2007). From stage 3 of flower development onward, some *SOC1* expression reappears in the central part of the floral meristem and later on in developing stamens and carpels, but at much lower levels than in the SAM at the floral transition. In conclusion, *SOC1* plays a pivotal role in the integration of multiple flowering signals and in maintaining meristematic activity in young floral meristems in a redundant manner with *AGL24* and *SVP* (Gregis et al., 2009; Liu et al., 2009). Altogether, this demands tight control of its activity by a plethora of different regulatory factors (for review, see Lee and Lee, 2010).

In this study, we unraveled part of the transcriptional regulatory network integrating SOC1 activity by the identification of upstream and downstream factors. We focused on the transition from vegetative to reproductive development, as at this transition point SOC1 functions both as an integrator of flowering signals and as a mediator of meristematic activity in the initiated floral meristems. Loci bound by SOC1 were identified by a ChIP-seq-based genome-wide target gene analysis, making use of a line in which a GFP-tagged version of SOC1 is expressed from its native regulatory sequences. For the identification of *SOC1* upstream regulators, a matrix-based yeast one-hybrid approach was employed. Because *SOC1* has been shown to be under the control of various other MADS domain proteins and these proteins are known to regulate each other's activity via complex regulatory loops (for review, see de Folter and Angenent, 2006), we focused on *SOC1* regulation by members of this TF family. In planta reporter-gene studies were used to determine the effects of the floral MADS domain proteins AP1, AGAMOUS (AG), and SEP3 on *SOC1* expression. Our results provide strong evidence for the down-regulation of *SOC1* in flowers by a number of floral MADS box proteins and attribute an important role to the SOC1 protein in its own repression. Furthermore, the important central role of SOC1 in flowering-time regulation is emphasized by the presence of a large number of well-known flowering-time regulators among SOC1's direct targets.

RESULTS

Complementation of *soc1-2* by *gSOC1:GFP*

SOC1 is an important regulator of the transition to flowering and integrates diverse flowering-time signals

in leaves and at the shoot meristem. To identify direct targets of SOC1, we created a C-terminal GFP-tagged 8.2-kb genomic construct (*gSOC1:GFP*) that was able to completely rescue the late flowering of the *soc1-2* mutant. Whereas the *soc1-2* mutant produced on average 19.0 ± 0.5 (2× SE) leaves under inductive long days at 23°C, transgenic mutant plants carrying either the *gSOC1:GFP* or the untagged *gSOC1* construct produced 12 ± 0.6 and 14 ± 0.4 leaves, respectively. The rescued mutants were indistinguishable from wild-type ecotype Columbia (Col-0) controls, which produced 12 ± 0.5 leaves before transitioning to flowering (Fig. 1, A and B). Next, we analyzed the expression domain of *gSOC1:GFP* by confocal microscopy. For this purpose, plants were initially grown under short-day (SD) conditions to keep them in the vegetative state. Under these conditions, SOC1:GFP signal is low in young leaf primordia and hardly detectable in the shoot meristem (Fig. 1C). Subsequently, the plants were transferred to LD conditions, resulting in a fast increase in SOC1 protein accumulation in the shoot meristem, and the transition to flowering occurs (Fig. 1, D–F). Already after 3 to 5 d in LD conditions, the switch to flowering is morphologically visible: the shoot meristem is enlarged and produces floral meristems on its flanks instead of leaves (Fig. 1, D and E). *SOC1* signal is absent from young stage 1 and 2 floral meristems (Fig. 1F), but signal reappears in the central region of the flower buds during later developmental stages (Fig. 1, F and G). In general, the observed SOC1:GFP localization follows the pattern described for *SOC1* mRNA (Lee et al., 2000; Samach et al., 2000). Taken together, these findings indicate that the genomic *SOC1* construct used in this study contains all elements required for *SOC1* expression and that the SOC1:GFP fusion protein is fully functional.

Genome-Wide Identification of *SOC1* Target Genes

To better understand the role of SOC1 in regulating the reproductive phase transition and during flower development, chromatin immunoprecipitation (ChIP) was performed in triplicate on transition apices isolated from *gSOC1;soc1-2* (control) and *gSOC1:GFP;soc1-2* lines. Isolated DNA was subjected to high-throughput sequencing, and after filtering for read quality, between 0.6 and 2.9 million sequencing reads per sample were uniquely mapped to The Arabidopsis Information Resource (TAIR) 10 genome (Supplemental Table S1). In total, 363 regions in the genome, representing putative binding sites, exhibited statistically significant enrichment in *gSOC1:GFP* over the control samples at a false

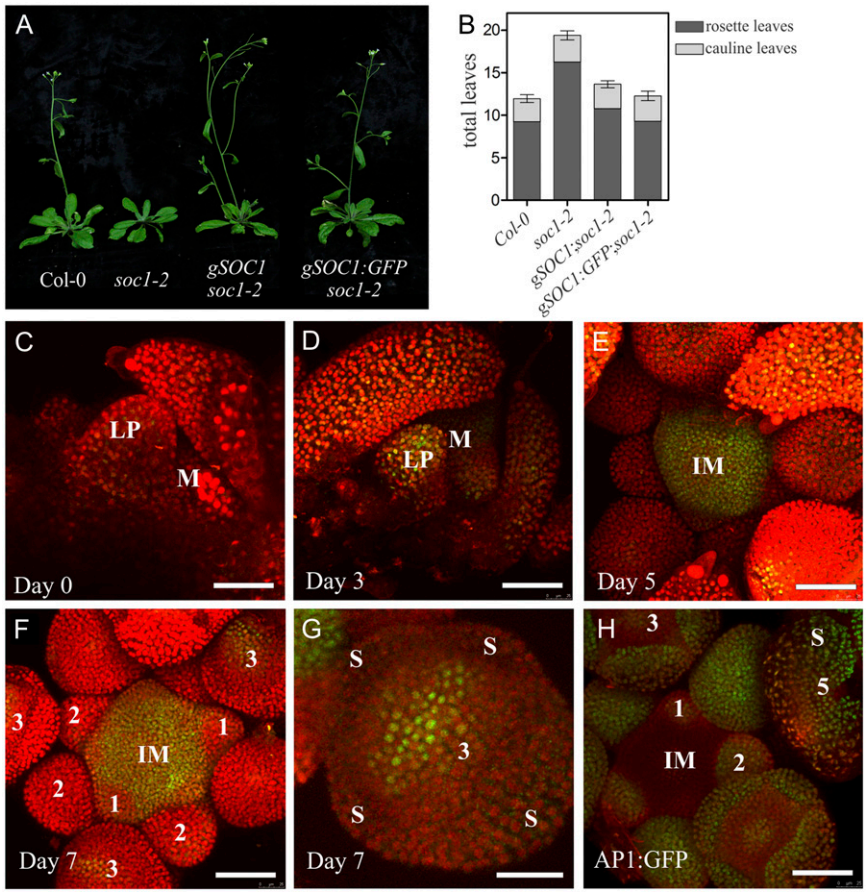

Figure 1. Analysis of gSOC1:GFP lines. A, Col-0, *soc1-2*, *gSOC1;soc1-2*, and *gSOC1:GFP;soc1-2* 30-d-old plants grown in LD conditions at 23°C. B, *gSOC1;soc1-2* and *gSOC1:GFP* lines show complementation of the *soc1-2* late-flowering phenotype. Error bars indicate 2× SE of the total leaf number. C to G, Analysis of SOC1 expression at the switch from vegetative to reproductive development in *gSOC1:GFP* transgenic plants. gSOC1:GFP signal is shown in green and pTUB6:TagRFP signal is shown in red. C shows SOC1 localization in the shoot meristem region of a representative 3-week-old plant grown under SD conditions and in the vegetative state of development. Subsequently, the plants were switched to LD conditions and SOC1 signal was imaged after 3 d (D), 5 d (E), and 7 d (F). G shows SOC1 expression in a stage 3 floral bud. Some signal reappears in the center of the floral meristem. H, AP1:GFP expression in an inflorescence at a developmental stage similar to F. IM, Inflorescence meristem; LP, leaf primordium; M, shoot meristem; S, sepal. Numbers 1 to 5 indicate floral meristem stages. Bars = 50 μm in C to F and H and 25 μm in G.

discovery rate (fdr) of 0.1 in all three biological replicates (Supplemental Table S2). In almost all of these regions of local enrichment (352), at least one protein-coding or microRNA gene could be identified within a distance of ±3 kb of the peak. Most of the peaks (281) were located in either the promoters or downstream regions of genes, and several (71) were associated with exons or introns. Only 11 peaks were not directly associated with genes (i.e. were more than 3 kb distant from an annotated gene; Supplemental Table S2). A MEME search for enriched sequence motifs in the 100 top-ranking peaks reveals the presence of a perfect consensus MADS domain TF-binding site (CArG box [de Folter and Angenent, 2006]; Fig. 2I).

Among the high-confidence genes bound by SOC1 (Fig. 2, A–H; Supplemental Table S3) were many TFs known to be involved in flowering-time regulation (Table I). Strikingly, the best-ranked peak obtained in the ChIP-seq experiment is located approximately 90 bp upstream of the *SOC1* 5′ untranslated region (UTR; Figs. 2A and 3C), indicative of strong feedback regulation of *SOC1* by its own gene product (see below). Besides *SOC1*, several other MADS box genes also showed binding by SOC1. These include the floral repressors *SVP*, *AGL15*, and *AGL18* (Fig. 2G; Adamczyk et al., 2007; Li et al., 2008). In addition to *SVP*, which regulates flowering in response to temperature (Lee et al., 2007), *SOC1* also targeted *CRT/DRE-BINDING FACTOR1* (*CBF1*), *CBF2*, and *CBF3* (Fig. 2B), proteins that contain AP2-like DNA-binding domains and that are involved in the response to low temperature. *SOC1* down-regulates *CBFs*, which induce the expression of the *SOC1* repressor *FLC*, generating a positive feedback loop that promotes *SOC1* expression under warm conditions (Seo et al., 2009). Besides the *CBF* genes, SOC1 was found to directly bind to regulatory regions

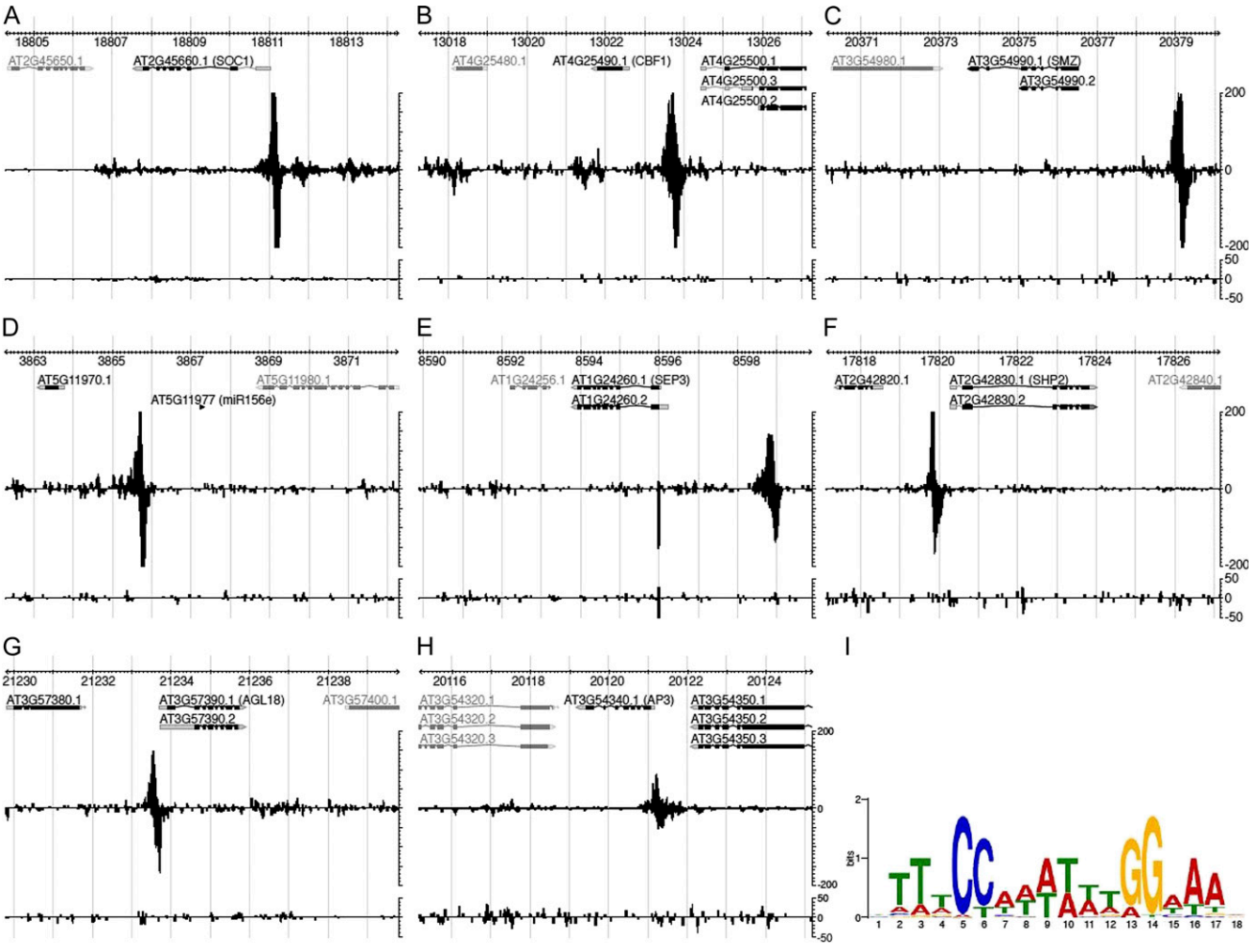

Figure 2. Targets of SOC1 identified by ChIP-seq. A to H, Examples of flowering-time and flower development loci directly bound by SOC1. The graphs in each panel show the local enrichment of SOC1 binding in *gSOC1:GFP;soc1-2* (top graph) over the control experiment (*gSOC1;soc1-2*; bottom graph). Chromosomal position (TAIR 10) and models of the genes flanking the peaks are given at the top of the panels. Each panel shows a 10-kb window centered around the flanking genes. I, CArG box motif overrepresented in the 100 top-ranking peaks. [See online article for color version of this figure.]

Table I. *Known and potential flowering-time and floral organ identity genes targeted by SOC1*

Above the boldface data line, all highly confident SOC1 binding positions are indicated. The binding events in and below the boldface line scored above the set threshold level in at least one of the three replicates.

Orp Rank[a]	Up/Down Gene No.[b]	Gene Name[c]	Genomic Position[b,d]	fdr Biological Replicate 1[e]	fdr Biological Replicate 2[e]	fdr Biological Replicate 3[e]
1	AT2G45660	*SOC1*	89	0	7.06E-155	6.17E-156
2	AT2G40805	*miR319c*	2,291	0	4.30E-158	5.12E-143
10	AT3G54990	*SMZ*	2,628	1.47E-167	5.80E-50	1.84E-36
14	*AT5G11977*	*miR156e*	*1,495*	9.29E-125	3.66E-43	2.74E-38
17	AT1G24260	*SEP3*	2,725	6.84E-125	8.49E-36	2.83E-26
26	*AT2G21070*	*FIO1*	*2,901*	3.27E-96	5.35E-23	4.34E-22
27	*AT2G42830*	*SHP2*	*374*	3.71E-72	1.11E-22	4.95E-26
31	*AT3G57390*	*AGL18*	*86*	5.77E-51	1.24E-23	5.67E-22
35	AT5G67180	*TOE3*	1,377	3.30E-42	1.47E-18	4.41E-24
63	*AT3G23130*	*SUP*	*956*	3.40E-33	6.62E-08	3.78E-12
85	AT2G33860	*ETT/ARF3*	2,406	5.49E-25	7.22E-06	3.36E-11
88	*AT4G36920*	*AP2*	*1,653*	2.53E-22	4.42E-10	4.55E-07
93	AT5G13790	*AGL15*	234	6.77E-26	2.35E-07	2.28E-05
99	AT3G54340	*AP3*	146	4.11E-29	4.65E-06	0.00011
120	*AT1G68840*	*TEM2*	*2,627*	3.06E-25	6.17E-06	0.00390
127	AT5G37260	*CIR1*	2,589	1.14E-16	0.00304	1.19E-07
151	AT1G09570	*PHYA*	518	1.56E-10	0.00067	0.00017
167	AT5G20240	*PI*	1,600	2.53E-18	0.00564	0.00678
216	AT2G39250	*SNZ*	871	1.08E-14	0.09177	0.00037
220	*AT4G39400*	*BRI1*	*1,827*	6.72E-15	0.00061	0.06837
248	*AT2G22540*	*SVP*	*2,248*	0.00277	0.00021	0.01839
273	*AT5G02030*	*PNY*	*2,635*	3.42E-09	0.00802	0.07193
399	**AT1G25560**	***TEM1***	**785**	**1.58E-06**	**0.32562**	**0.00407**
460	*AT1G53230*	*TCP3*	*1,187*	4.45E-06	0.28021	0.02362
480	AT4G32980	*ATH1*	153	0.00076	0.26590	0.01159
510	AT3G47500	*CDF3*	1,832	0.07417	0.08909	0.01199
567	AT2G28550	*TOE1*	97	8.95E-06	0.30502	0.05613
919	*AT1G54830*	*NFYC9*	*26*	0.01235	0.31815	0.09357
1241	*AT5G41663*	*miR319b*	*690*	0.09056	0.62522	0.01219

[a]Rank of the binding peak based on the product of the *P* value ranks for the three replicates. [b]All downstream events are italic, and all upstream events are roman. [c]Gene name abbreviations not defined in the text: *BRI1, BRASSINOSTEROID INSENSITIVE1*; *PNY, PENNYWISE*; *TEM1, TEMPRANILLO1*; *ATH1, ARABIDOPSIS HOMEOBOX1*; *CDF3, CYCLING DOF FACTOR3*; *NFYC9, NUCLEAR TRANSCRIPTION FACTOR Y SUBUNIT C-9*. [d]Distance of the closest genes upstream/downstream from the center of the peak. [e]Benjamini-Hochberg adjusted fdr of the peak.

of a number of other *AP2*-like genes involved in flowering-time regulation, such as *TEMPRANILLO2* (*TEM2*; Castillejo and Pelaz, 2008), *AP2*, *TARGET OF EAT3* (*TOE3*), *SCHLAFMüTZE* (*SMZ*; Fig. 2C), and *SCHNARCHZAPFEN* (*SNZ*; Aukerman and Sakai, 2003; Mathieu et al., 2009).

Apart from regulators of flowering time, SOC1 also binds to the regulatory regions of several floral homeotic genes, such as the MADS box genes *SEP3* (Fig. 2E), which is one of the most strongly enriched SOC1 targets, *AP3* (Fig. 2H), *PISTILLATA* (*PI*), and *SHATTERPROOF2* (*SHP2*; Fig. 2F). In addition, the zinc-finger TF gene *SUPERMAN* (*SUP*), which is involved in the control of cell proliferation in stamen and carpel primordia and in ovules (Ito et al., 2003), is bound by SOC1. The same holds for *AUXIN RESPONSE TRANSCRIPTION FACTOR3* (*ARF3/ETTIN*), which imparts regional identity in the floral meristems affecting perianth organ number spacing, stamen formation, and regional differentiation in stamens and gynoecium (Sessions et al., 1997).

To verify the quality of our ChIP-seq data set, the list of highly confident targets (Supplemental Table S3) was compared with a recently published genome-wide SOC1 target gene list (Tao et al., 2012). It is important to realize that we identified SOC1 targets by a ChIP-seq approach at the moment of transition from vegetative to reproductive development and that *SOC1* was expressed from its native regulatory sequences. In contrast, Tao et al. (2012) identified SOC1 targets in 9-d-old seedlings using a ChIP-chip approach and a *SOC1* overexpression line. It is well known that MADS domain TFs act in a dynamic manner and can have different target genes depending on the developmental stage, as was shown for AP1 (Kaufmann et al., 2010b). Nevertheless, almost 30% of the SOC1 target genes (130 out of 474) identified by Tao et al. (2012) were also identified in our screen. A subsequent Biological Networks Gene Ontology analysis for overrepresented plant ontology terms (Maere et al., 2005) revealed the overrepresentation of genes supposed to be involved in "response to stress," "response to endogenous stimulus," and "response to external stimulus" in the 130 commonly identified SOC1 targets (fdr = 0.05). These overrepresented ontology classes include, for example, genes involved in the floral timing pathways. The

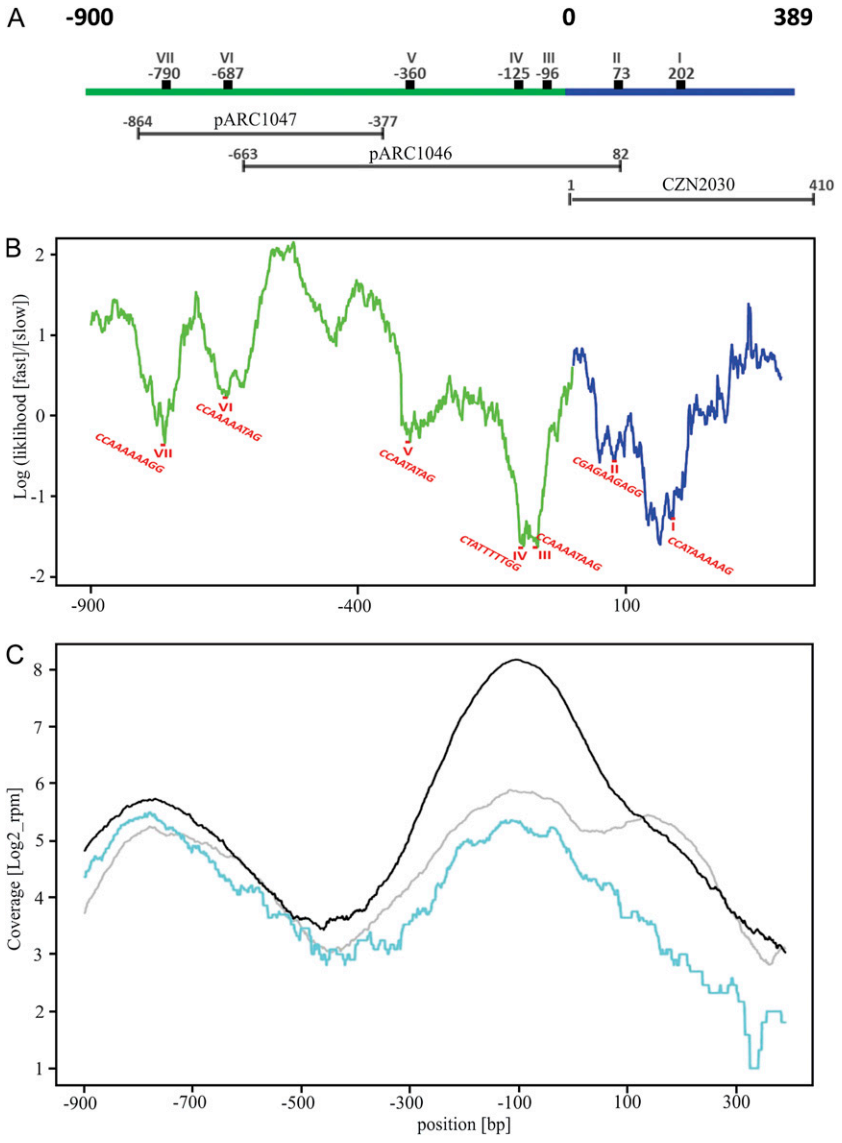

Figure 3. Genomic structure and regulation of the *SOC1* locus. A, Schematic representation of the Arabidopsis *SOC1* promoter region and 5′ UTR. The numbering is relative to the first position of the 5′ UTR sequence (position 0). The 5′ UTR is indicated in blue, and the upstream promoter region is indicated in green. The positions of seven putative CArG box sequences are indicated. The three fragments that have been used for the yeast one-hybrid assays (pARC1046, pARC1047, and CZN2030) are presented below the schematic representation of the *SOC1* upstream region. B, Likelihood ratios under a fast- versus slow-mutation regime for the Arabidopsis *SOC1* upstream genomic region. The *x* axis represents the position in the sequence, and the *y* axis represents the log-likelihood ratio at that position. A relative lower ratio indicates a higher degree of constraint on the mutability of that position. The numbers in red represent perfect matches with the CArG box ($CC[W]_6GG$) and CArG box-like ($C[W]_7GG$, $CC[W]_7G$, and $C[W]_6G$) consensus sequences, located in slow-mutated regions that overlap with AP1, SEP3, or SOC1ChIP-seq binding regions. C, Chip-seq scores (peaks) for AP1, SEP3 (Kaufmann et al., 2009, 2010b), and SOC1 are shown by the lines in gray, blue, and black, respectively.

ontologies "postembryonic development" and "flower development" were only overrepresented in our ChIP-seq data set (fdr = 0.05). This observation reflects well the difference in sampled material, in which we used apices in the transition from vegetative to reproductive development or just switched to flower development.

In order to obtain evidence for the transcriptional regulation of genes that are bound by SOC1 in our ChIP-seq experiments, we initially analyzed a publicly available microarray data set representing the transcriptional effects of *SOC1* overexpression (Seo et al., 2009). This analysis shows differential expression for about 50 of the genes bound by SOC1 in our genome-wide target gene analysis (Supplemental Table S3). Subsequently, a number of putative SOC1 target genes were selected, and quantitative reverse transcription-PCR was performed to show the differential expression of these genes comparing wild-type Col-0 plants, *pCaMV35S:SOC1* overexpression plants, and *soc1-2* mutant plants grown under the same conditions as used in the ChIP-seq experiments (3-d LD induction; Supplemental Fig. S1). These analyses reveal a SOC1-dependent response of the analyzed putative target genes that is in accordance with the functions of *SOC1* and these genes. Taken together, our ChIP-seq data demonstrate that SOC1 binds to the regulatory sequences of numerous important flowering-time and flower developmental genes. These findings confirm the importance of SOC1 as a central integrator of flowering-time signals but also highlight the role of SOC1 at later stages of flower development.

Characterization of *SOC1* Regulatory Sequences

Because of the central role of *SOC1* as a flowering-time regulator, its expression is under the tight control of

a plethora of flowering-time signals. At the molecular level, this is, among others, enforced by various MADS domain TFs (Hepworth et al., 2002; Liu et al., 2007, 2008; Li et al., 2008). Additionally, our ChIP-seq analysis shows binding of the *SOC1* locus by SOC1 itself (Figs. 2A and 3C). Analysis of the *SOC1* genomic region upstream of the translational start site reveals the presence of a number of consensus binding sites for MADS domain proteins (CArG box [Treisman, 1986; Shore and Sharrocks, 1995]; Fig. 3, A and B). In order to unveil the conservation of these and other putative binding sites, we applied phylogenetic footprinting (Fig. 3B) to the promoter regions of *SOC1* orthologs from seven eudicot species (Supplemental Fig. S2). This analysis revealed the presence of various regions with a local higher degree of constraint on mutability, suggesting selection pressure. Remarkably, in the majority of these conserved regions, a CArG box was located in the center of the peak, providing additional evidence for the importance of *SOC1* regulation by MADS domain proteins.

Identification of *SOC1* Upstream Regulators

A large number of known *SOC1* regulators belong to the MADS domain TF family, whose members are known to bind DNA as dimers (Huang et al., 1996; Riechmann et al., 1996). Based on this knowledge, we performed a comprehensive matrix-based yeast one-hybrid assay to identify MADS domain proteins that are able to bind *SOC1* regulatory sequences. For this purpose, all type II MADS domain protein dimers (135) were selected from the available Arabidopsis MADS dimer collection in yeast (Immink et al., 2009). This subset of dimers was screened in a modified yeast one-hybrid assay against two different *SOC1* promoter fragments (pARC1046 and pARC1047) and a *SOC1* 5′ UTR fragment (CZN2030; Figs. 3A and 4). As shown in Figure 4 and Supplemental Table S4, specific binding was obtained for all fragments tested. Because of the setup of the yeast one-hybrid assay, we cannot rule out that in some cases only the MADS domain protein expressed as a GAL4-AD fusion protein is bound to the regulatory DNA sequence as a homodimer. Nevertheless, in most cases, differences in binding were obtained depending on the second MADS domain protein that is expressed from the pTFT1 vector, which strongly suggests binding by a multiprotein complex consisting of two MADS domain proteins expressed in yeast. In line with the ChIP-seq data, we could identify binding of dimers containing the SOC1 protein to the *SOC1* proximal promoter fragment and 5′ UTR.

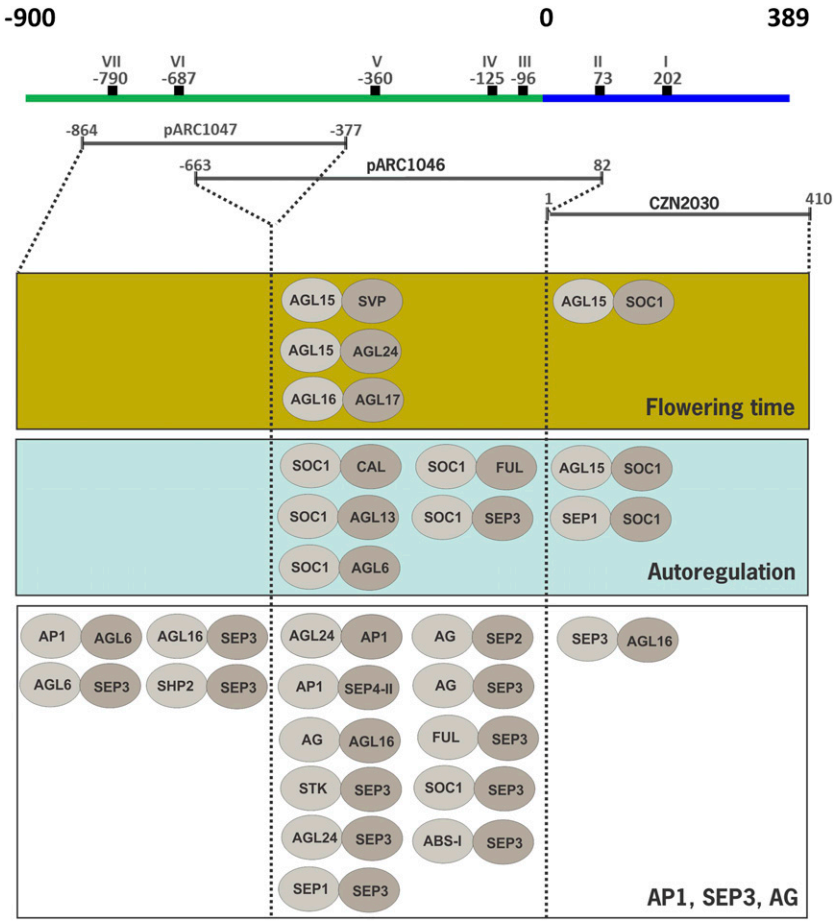

Figure 4. Binding of *SOC1* regulatory sequences by particular MADS domain protein dimers. The drawing at the top represents the *SOC1* upstream sequence (promoter and 5′ UTR). Below that, the three fragments are indicated that were used in the yeast one-hybrid assay (pARC1046, pARC1047, and CZN2030). Only dimers of MADS domain proteins involved in flowering-time regulation or floral organ identity specification are shown. MADS domain protein dimers binding to the indicated *SOC1* regulatory sequences have been categorized according to their supposed function (flowering time, autoregulation, or control of *SOC1* inside flowers mediated by AP1, SEP3, or AG). For a complete overview of *SOC1* yeast one-hybrid results, see Supplemental Table S4. [See online article for color version of this figure.]

Furthermore, complexes consisting of proteins involved in floral timing and transition are binding to the *SOC1* regulatory sequences (e.g. SVP-AGL15 and FRUITFUL-SOC1). Remarkably, a large number of interactions also are found with complexes consisting of "ABC-class" MADS domain proteins involved in floral organ specification (e.g. AG-SEP3) and complexes consisting of a protein involved in floral transition and a protein that plays a role in floral organ development (e.g. AGL24-AP1 and SOC1-SEP3). Previously, it was shown that AP1 is involved in the repression of *SOC1* in the floral meristem (Liu et al., 2007). Our yeast one-hybrid data confirm the binding of AP1 in combination with particular dimerization partners to the *SOC1* promoter. In addition, our yeast one-hybrid data suggest a role for other floral homeotic MADS domain proteins in *SOC1* regulation directly after the switch to reproductive development or during later steps of flower development.

Repression of *SOC1* Expression by Floral MADS Domain TFs

To study in more detail the relevance of the identified binding to *SOC1* regulatory sequences by ABC-class MADS domain proteins, in planta reporter assays were performed. Transgenic lines that constitutively express Glucocorticoid Receptor (GR) domain fusion proteins with AP1 (Wellmer et al., 2006), SEP3 (Kaufmann et al., 2009), or AG were crossed to a homozygous line containing the *GUS* reporter gene driven by a *SOC1* promoter fragment referred to previously as the 1-kb *SOC1* promoter (positions −966 to +960; Hepworth et al., 2002). Subsequently, lines homozygous for both transgenes were selected in the F2 generation. The activity of the *SOC1* promoter was analyzed in 10-d-old seedlings obtained from these crosses grown on solid medium with and without induction by dexamethasone (DEX) under LD conditions. In addition, seedlings were grown for 9 d on medium without induction and transferred afterward to plates supplemented with DEX. After incubation for 1 d on this inductive medium, a GUS assay was performed. The GR-fused MADS domain proteins are expected to enter the nucleus and to become functional upon DEX treatment (Sablowski and Meyerowitz, 1998). Under noninductive conditions, the 1-kb *SOC1* promoter appears to be active in all tissues from 10-d-old seedlings (Fig. 5), with the strongest expression in the SAM region, as shown previously (Hepworth et al., 2002). The control experiments with only the reporter construct in the Col-0 background revealed that DEX treatment as such does not have a substantial effect on *SOC1* promoter activity levels or its pattern of activity in seedlings. In contrast, expression of the *SOC1* reporter is strongly reduced upon the activation of AP1, SEP3, or AG by DEX. Note that seedlings from the *AP1*:*GR* line growing continuously on DEX medium are smaller and that seedlings from *SEP3*:*GR* and *AG*:*GR* lines growing on the DEX medium have very small and curled leaves. These phenotypic alterations can be attributed to the ectopic expression of the respective MADS box genes and are in agreement with previous reports (Mizukami and Ma, 1992; Mandel and

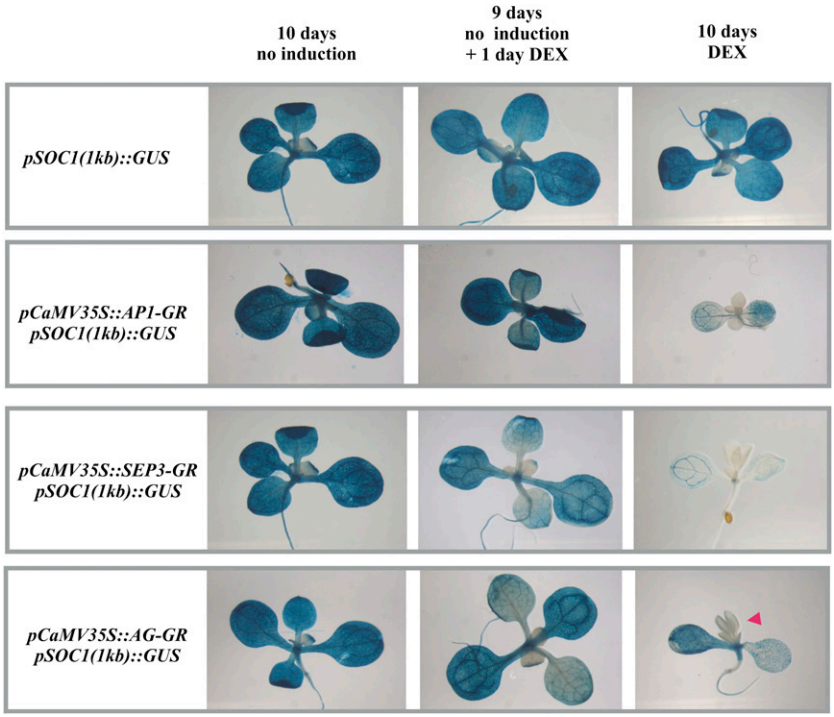

Figure 5. Repression of *SOC1* expression by AP1, SEP3, and AG. Expression of the *GUS* reporter gene driven by the 1-kb *SOC1* promoter (Hepworth et al., 2002) was analyzed separately or in combination with *pCaMV35S*::*AP1*:*GR*, *pCaMV35S*::*SEP3*:*GR*, or *pCaMV35S*::*AG*:*GR* constructs. The GUS assays were performed on seedlings of the respective lines after 10 d of growth on 0.5 MS, 9 d on 0.5 MS plus 1 day on 0.5 MS supplemented with DEX, or 10 d on 0.5 MS supplemented with DEX. From each treatment × plant line combination, one representative seedling is shown. Note that GUS is a stable protein and represents repression with a delay. The red arrowhead indicates the repression of *SOC1* by AG in the first true leaves.

Yanofsky, 1995; Honma and Goto, 2001). Previously, it was shown that AP1 is indeed able to repress *SOC1* in early floral meristems (Liu et al., 2007). To obtain further evidence for the repression of SOC1 by SEP3 and AG, additional DEX treatments were performed on these specific lines at the moment of the transition to reproductive development. For this purpose, plants were grown in SD conditions for 3 weeks and subsequently induced to flower by transfer to LD conditions. At the same time, the plants were treated with DEX, and this treatment was repeated daily. Three days after the switch, a GUS assay was performed revealing the repression of *SOC1* promoter activity by AG and SEP3 at this developmental stage (Supplemental Fig. S3). All together, the in planta reporter assays show that the floral homeotic MADS domain proteins AP1, SEP3, and AG are able to repress *SOC1*.

In Vivo Binding of MADS Domain TFs to the *SOC1* Promoter Region

Combining the yeast one-hybrid assay results (Fig. 4; Supplemental Table S4) with the results of the reporter assays (Fig. 5; Supplemental Fig. S3) suggests that the analyzed floral MADS domain proteins repress *SOC1* expression by direct binding to its upstream regulatory sequences. Previously, Liu et al. (2007) showed that this is in fact the case for AP1. They made use of ChIP followed by quantitative PCR (qPCR) to identify protein-bound genomic regions. Recently, we performed genome-wide target gene analyses for the AP1 and SEP3 proteins by ChIP-seq, which confirmed the binding of AP1 and identified SEP3 as an additional binding factor of the *SOC1* locus (Fig. 3C; Kaufmann et al., 2009, 2010b). One of the CArG box sequences in the *SOC1* promoter region, designated "CArG box III" (Fig. 3A), appears to be directly bound by AP1 and SEP3 and also by the floral repressor MADS domain protein FLC (Hepworth et al., 2002). Further analyses of a *SOC1*-reporter construct with mutations in this binding site indicated a pivotal role for this CArG box in the down-regulation of *SOC1* expression by FLC during the vegetative stage of development in nonvernalized plants (Hepworth et al., 2002). These observations led us to hypothesize that CArG box III might be a central mediator of *SOC1* repression, including its repression in floral meristems. To test this hypothesis, we analyzed the activity of the wild-type 1-kb *SOC1* promoter and the expression of *pSOC1*(1kb)*ΔCArG-III*::*GUS* inside flowers (Hepworth et al., 2002). The intact promoter element gives weak reporter gene expression in the anther locules, whereas all other full-grown floral tissues contain hardly any GUS signal (Fig. 6A). In contrast to this weak and restricted GUS signal, reporter lines with the mutated CArG-III sequence appear to give substantial floral expression (Fig. 6B). In these transgenic lines, strong *GUS* expression was obtained in sepals, anther filaments, and style and stigma tissues. This result supports the idea that CArG-III is important for limiting *SOC1* expression inside floral tissues.

Autoregulatory Feedback Loops for *SOC1* Repression

We postulated previously that down-regulation of flowering time genes inside the flower is mediated by MADS domain protein complexes consisting of floral timing MADS domain proteins, such as SOC1, and floral organ identity proteins, such as AP1 (de Folter et al., 2005). Autoregulatory feedback loops are common for plant MADS domain proteins, and well-known examples are the feedback loops involved in the maintenance of expression for the B-type MADS box genes (Schwarz-Sommer et al., 1992; Tröbner et al., 1992; Goto and Meyerowitz, 1994; Jack et al., 1994), for the C-type gene *AG* (Gómez-Mena et al., 2005), and for the E-type gene *SEP3* (Kaufmann et al., 2009). Elaborating on this postulated hypothesis, we expect that the repression of *SOC1* by the ABC-class MADS domain proteins is dependent on a complex consisting of SOC1 and the floral homeotic MADS domain proteins. Indeed, various dimers and higher order complexes have been identified containing these proteins (de Folter et al., 2005; Immink et al., 2009), and the ChIP-seq experiments and yeast one-hybrid assays showed binding of the *SOC1* locus by at least AP1, SEP3, and SOC1 itself, in combination with a variety of dimerization partners (Figs. 3C and 4; Supplemental Table S4). To provide further evidence for the proposed role of the SOC1 protein in repressing its own expression, in combination with floral homeotic MADS domain proteins, in planta reporter assays were performed in a *soc1-6* mutant background (Fig. 6C). For this purpose, the homozygous lines described before, containing the *pSOC1*(1kb)::*GUS* reporter in combination with a *pCaMV35S*::*MADS*:*GR* construct, were introgressed into the *soc1-6* T-DNA insertion line. Subsequently, GUS assays were performed on plants from the selected lines that had been grown on standard medium or medium supplemented with DEX (Fig. 6C). Both AP1 and AG appeared to down-regulate the *SOC1* promoter only when the wild-type *SOC1* allele is present (compare Figs. 5 and 6C). In contrast, the SEP3 protein can apparently act on the *SOC1* promoter independently of SOC1, because the *pSOC1*-reporter construct is still down-regulated in a *soc1* mutant background (Fig. 6C). We then investigated whether CArG box III is essential for the repression of *SOC1* by SEP3 and crossed the *pSOC1*(1kb)*ΔCArG-III*::*GUS* construct into the *pCaMV35S*::*SEP3GR*;*soc1-6* background. In this case, no down-regulation could be obtained for the *GUS* reporter upon DEX treatment (Fig. 6D), showing that this binding site is essential for SEP3 protein-mediated repression of the *SOC1* promoter in vivo. These experiments provide strong evidence for the presence of negative autoregulatory loops, in which SOC1 represses its own expression in combination with AG and AP1.

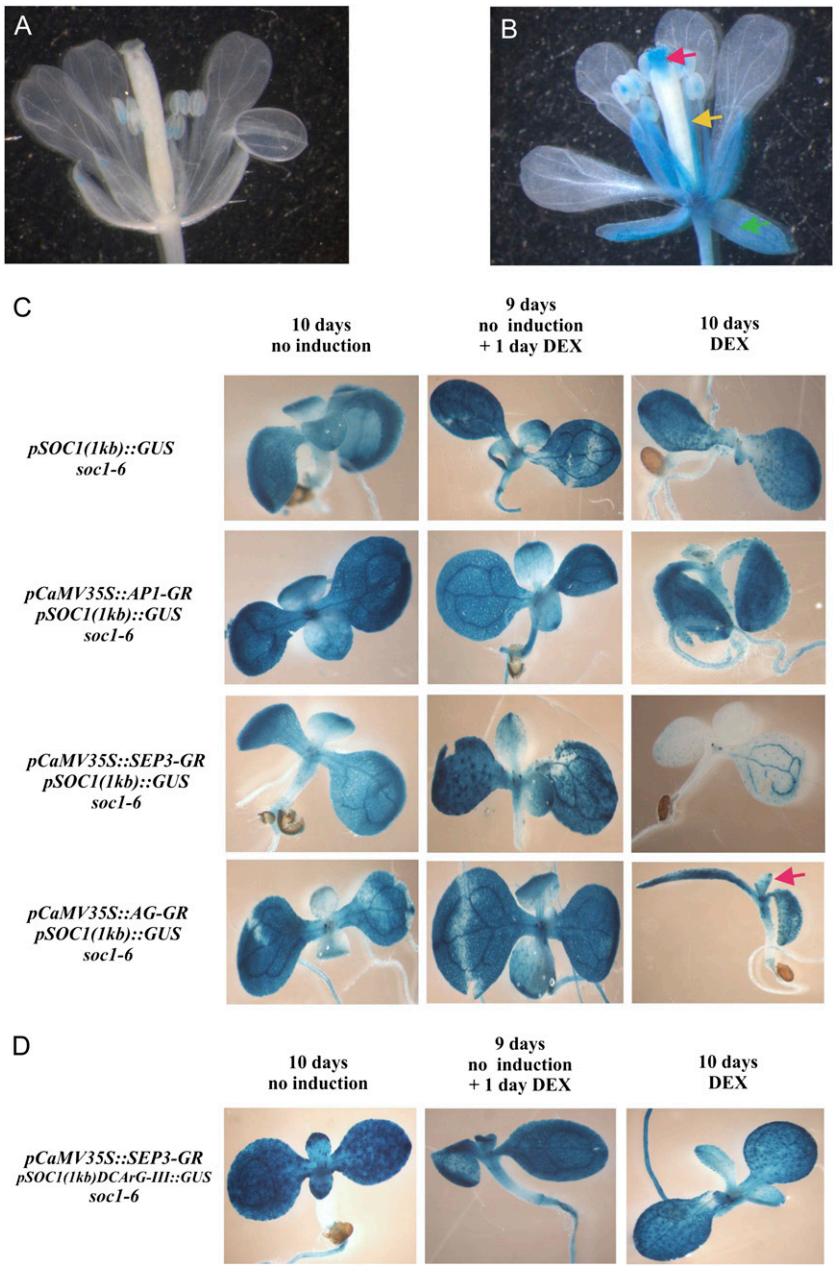

Figure 6. Role of CArG box III and dependency on SOC1 for *SOC1* repression by floral MADS domain proteins. A, Expression of *pSOC1(1kb)*::*GUS* in floral organs. B, Expression of *pSOC1(1kb)ΔCArG-III*::*GUS* in floral organs. Note the ectopic expression in sepals (green arrowhead), anther filaments (yellow arrowhead), and style and stigma tissues (red arrowhead). C, Expression of the *GUS* reporter gene driven by the 1-kb *SOC1* promoter fragment (Hepworth et al., 2002) in the *soc1-6* mutant background and in *soc1-6* mutant seedlings containing the *pCaMV35S*::*AP1*:*GR*, *pCaMV35S*::*SEP3*:*GR*, or *pCaMV35S*::*AG*:*GR* construct. The GUS assays were performed on seedlings of the respective lines after 10 d of growth on 0.5 MS, 9 d on 0.5 MS plus 1 d on 0.5 MS supplemented with DEX, or 10 d on 0.5 MS supplemented with DEX. From each treatment × plant line combination, one representative seedling is shown. D, Expression of the *GUS* reporter gene driven by a 1-kb *SOC1* promoter fragment containing a mutation in CArG box III (see Fig. 3) in the *soc1-6/pCaMV35S*::*SEP3*:*GR* background. Seedlings were grown on the same media as in C.

DISCUSSION

In this study, we unraveled part of the regulatory network controlling the *SOC1* gene and target genes being controlled by the SOC1 MADS domain TF. *SOC1* is one of the key integrating factors of flowering-time signals and, hence, translates input from the various flowering-time pathways into a unique flower-inducing signal (Lee and Lee, 2010). After fulfilling this role as hub in the network and shortly after the switch from vegetative to reproductive development, it is of importance that *SOC1* activity is repressed to avoid the malformation of flowers, which would result in a negative effect on plant fitness (Borner et al., 2000).

SOC1 Is at the Center of the Flowering-Time Regulatory Network

SOC1 is known as an integrator of different flowering-time signals and, therefore, is placed genetically at the end of the floral timing gene cascade (Lee and Lee, 2010). However, SOC1 also binds numerous key flowering-time regulatory genes (summarized in Table I; Tao et al., 2012), which genetically are supposed to act upstream of *SOC1* and for which in some cases direct binding of the encoded protein to the *SOC1* locus has been shown. For example, SOC1 binds to the regulatory regions of the floral repressors *AP2*, *TOE3*, *SMZ* (Fig. 2C), and *SNZ*, four of the six TFs with a

miR172 target site in the Arabidopsis genome. These TFs constitute an important group of floral repressors, where AP2 and SMZ have been shown to bind to the *SOC1* locus, resulting in its repression (Mathieu et al., 2009; Yant et al., 2010). As expected, the performed expression studies revealed that SOC1 is able to repress the expression of this group of *AP2* TFs (Supplemental Fig. S1; Tao et al., 2012). Furthermore, and similar to AP2 (Yant et al., 2010), SOC1 targets *MIR156e* (Wang et al., 2009), which indirectly regulates *AP2* expression via the *SPL* and *MIR172* genes. AGL15 is another floral repressor that binds the *SOC1* locus (Supplemental Table S4; Zheng et al., 2009), which is also targeted by SOC1. In addition, *AGL15* is under the control of AP2, which activates its expression and adds an additional layer of regulatory complexity (Yant et al., 2010). Besides *AGL15*, SOC1 binds to other flowering-time repressor loci belonging to the MADS domain TF family, such as *SVP* and *AGL18* (Table I), both of which seem to be repressed by SOC1 (Supplemental Fig. S1). Based on these findings and the antagonistic expression patterns of the floral repressors and *SOC1* during the vegetative stage of development (Schmid et al., 2005), it is tempting to speculate that SOC1 is repressing the majority of its own repressors. This type of double-negative feedback loop is frequently observed in developmental pathways and serves as a molecular switch with two steady states: either the flowering repressors are on and *SOC1* is off, or the opposite (Alon, 2007). A (transient) signal, which could be a flowering-inducing factor or reaching a particular temperature, could induce *SOC1* above a threshold level, after which the network irreversibly and independently of the signal locks into the flowering state (*SOC1* on) by suppressing the repressors. In summary, SOC1 binds loci of a large number of known flowering-time regulators (Table I), which places *SOC1* molecularly in the center of the flowering regulatory network. Furthermore, our ChIP-seq and expression analysis data suggest that this network contains multiple regulatory loops and feedback mechanisms.

SOC1 Binds Loci with a Potential Role in Flowering Time Regulation

In addition to the well-described flowering-time regulators discussed above, SOC1 binds loci encoding genes with a potential role in the flowering response. One example is *SMALL UBIQUITUN-LIKE MODIFIER3* (*SUM3*), which belongs to a small gene family of ubiquitin-like posttranslational modifiers (van den Burg et al., 2010). In contrast to single mutants for *SUM1* or *SUM2*, *sum3* plants appear to be late flowering, whereas overexpression of *SUM3* results in early flowering. Based on this knowledge and the ChIP-seq data, one could assume that SOC1 binding of *SUM3* results in *SUM3* induction and hence a flowering-stimulating signal. Besides these examples for protein-coding genes, SOC1 appears to bind the loci of various microRNA genes, such as the above-mentioned *MIR156e*. Interestingly, another microRNA gene, *MIR319c*, was the second-best overall target of SOC1. miR319 and some of their targets, the *TEOSINTE BRANCHED1, CYCLOIDEA, AND PCF TRANSCRIPTION FACTORS* (*TCP*) genes, have been shown to be expressed in the developing flower (Cubas et al., 1999; Wellmer et al., 2006; Nag et al., 2009). Besides MIR319c, SOC1 also binds to regulatory sequences of the miR319 target *TCP3*, which is expressed throughout the young floral meristem at floral stages 2 and 3 and is more restricted to the sepal primordia at stage 4 (Cubas et al., 1999; Wellmer et al., 2006). As the expression pattern of *TCP3* is complementary to that of *SOC1*, SOC1 might repress *TCP3* in the developing flowers, both directly and indirectly via *MIR319c*. Additionally, plants ectopically expressing *MIR319a* show a late-flowering phenotype (Palatnik et al., 2003; Schommer et al., 2008), suggesting that the *miR319* targets play a role in floral timing as well, which could also in part be under the control of SOC1.

A Direct Role for SOC1 in the Repression of the Floral Homeotic MADS Box Genes?

Previous studies revealed the importance of maintaining *SEP3* and the B- and C-class floral organ identity genes in a suppressed state in the inflorescence meristem and young floral meristems (Liu et al., 2009). The repression in very young flowers is key to avoiding a precocious differentiation of the floral meristem during the first stages of development. SVP seems to play a major role in this, although SOC1 and AGL24 also have been shown to be important (Gregis et al., 2008; Liu et al., 2009). Our ChIP-seq data suggest an alternative mechanism, in which SOC1 directly represses the B-class genes *AP3* and *PI* in the inflorescence and flower meristems to prevent premature floral meristem differentiation. It seems that SOC1, SVP, and AGL24 jointly provide the floral meristem a short lag time in which differentiation is suppressed, allowing the establishment of sufficient cells for the inner floral whorls, from which the important reproductive organs will develop.

SOC1 Repression in Young Developing Floral Meristems

Analysis of *SOC1* expression at the mRNA (Samach et al., 2000) and protein (Fig. 1) levels reveals that its expression in developing young floral meristems is turned off, in contrast to the maintained strong SOC1 signals in the inflorescence meristem. This expression pattern is fully complementary to the expression of the floral meristem identity gene *AP1* (Fig. 1H) and can be explained by the direct repression of *SOC1* by AP1 (Liu et al., 2007). Here, we show that in addition to AP1, the floral organ identity proteins SEP3 and AG have the

potential to repress SOC1 as well. *SOC1* repression by multiple factors allows robust control over this gene during early flower development. However, despite the potential repression of *SOC1* by SEP3 and AG, some *SOC1* expression reappears during later stages of flower development in the center of the floral meristem (Fig. 1G). This suggests that *SOC1* repression by SEP3 and AG is less rigorous than repression by AP1 in the perianth primordia or, alternatively, that competing inducing factors cause some *SOC1* expression in the center of developing flowers. Nevertheless, the facts that *SOC1* is expressed only at low levels in full-grown flowers in part of the anthers (Fig. 6A) and that a mutation of CArG box III results in ectopic *SOC1* expression in anther filaments and stylar tissue (Fig. 6B) suggest that *SOC1* expression is actively repressed in later stages of whorl 3 and 4 development. Based on our results, SEP3 and AG, in combination with specific dimerization partners, are possible candidates for this function. A difference in *SOC1* repression by AP1, SEP3, and AG is seen in the dependence on the SOC1 protein itself. Both AP1 and AG appear to depend fully on SOC1 for the repression of *SOC1*. In contrast, SEP3 is able to repress *SOC1* expression in the absence of the SOC1 protein. The latter might be explained by differences in protein complex formation capacity: SEP3 has a large number of interaction partners and is able to interact with various flowering-time-regulating MADS domain proteins, such as AGL24 and SVP (de Folter et al., 2005; Immink et al., 2009). Based on this knowledge, we hypothesize that the role of SOC1 in *SOC1* repression by SEP3 can be taken over by another interacting MADS domain protein. In line with this hypothesis, we saw various SEP3 dimers binding the SOC1 regulatory sequences in our yeast one-hybrid assay (Fig. 4; Supplemental Table S4). The negative autoregulation, as shown here for SOC1, is a core transcriptional network component that is often seen in developmental regulatory networks to facilitate fast switches (Rosenfeld et al., 2002). Such an adequate and fast response is essential for *SOC1* suppression just after transition to the reproductive stage, where a rapid succession of developmental transitions take place. Analysis of the existence of autoregulatory loops shows conservation and overrepresentation of this network motif in various kingdoms, suggesting that this motif has been maintained in evolution (Kiełbasa and Vingron, 2008).

Molecular Mode of Action for *SOC1* Repression by SOC1 and Floral Homeotic MADS Domain Proteins

A remaining question is what is the exact stoichiometry and composition of the transcriptional repression complex in the negative autoregulatory *SOC1* loop. MADS domain proteins are able to bind DNA as dimers; hence, the most simple molecular unit for the *SOC1* negative feedback loop would be a heterodimer consisting of, for example, SOC1 and AP1. Yeast two-hybrid experiments reveal that SOC1-AP1 and SOC1-SEP3 dimers potentially can be formed (de Folter et al., 2005). Although SOC1-SEP3ΔC (dimer 283) appears to bind the proximal *SOC1* promoter region in yeast, this dimer is not exclusively responsible for the down-regulation of *SOC1*. In contrast, no binding could be detected for the SOC1-AP1 dimer (dimer 46; Supplemental Table S4), while we know from the reporter studies that the *SOC1* suppression by AP1 is SOC1 dependent (Fig. 6). Taking into account the capacity of plant MADS domain proteins to assemble into multimeric complexes, it might be that *SOC1* gets repressed by a higher order complex consisting of at least one SOC1 dimer and one AP1 dimer binding to the proximal *SOC1* promoter region. Identification of SOC1 and AP1 in the same protein complex isolated from native inflorescence material shows that these two proteins assemble into complexes in vivo (Smaczniak et al., 2012). The fact that AG is not found as a dimerization partner of SOC1 in yeast (de Folter et al., 2005) but interacts with SOC1 in a higher order complex (Immink et al., 2009) suggests that a similar model could hold for *SOC1* repression by the combination of AG and SOC1. Alternatively, the ABC-MADS domain proteins and SOC1 bind the regulatory sequences independently, and both binding events are essential for *SOC1* repression. A careful analysis of the ChIP-seq peaks for AP1 (Kaufmann et al., 2010b), SEP3 (Kaufmann et al., 2009), and SOC1 shows that the *SOC1* locus is bound at various positions by these proteins or their interaction partners; hence, different combinations of CArG boxes, including CArG box III, could be involved in mediating SOC1 repression. In the latter case, it is expected that the DNA from the *SOC1* promoter loops around such a higher order transcriptional repression complex. In both scenarios, the question remains whether additional general transcriptional repressors are essential. The repression of *SEP3* by SOC1 is mediated by at least two chromatin regulators, TERMINAL FLOWER2/LIKE HETEROCHROMATIN PROTEIN1 and SAP18 (Liu et al., 2009). Furthermore, different chromatin regulators were identified in the protein complex isolations for the floral homeotic MADS domain proteins (Smaczniak et al., 2012), supporting the idea that cofactors with transcriptional repression activity play a role in this type of negative feedback loop.

A Complex Regulatory Network of MADS Proteins in Flower Development

Genome-wide target gene analyses for a number of MADS domain proteins that control flowering time (Zheng et al., 2009; Deng et al., 2011; Tao et al., 2012) and floral organ identities (Gómez-Mena et al., 2005; Kaufmann et al., 2009, 2010a, 2010b) reveal that these master regulators target a large number and wide variety of genes, ranging from other regulatory factors to structural genes. Furthermore, these TFs control themselves and each other via direct regulatory interactions,

resulting in a complex interconnected network. Like *SOC1*, *AGL24* and *SVP* also are directly repressed by AP1 (Liu et al., 2007), SEP3, and AG (Gregis et al., 2008). All together, these results show that a tightly controlled balance exists between the activity and functioning of floral timing and floral organ identity-specifying MADS TFs around the transition from vegetative to reproductive development, resulting in a robust phase switch and the development of flowers and reproductive organs under optimal environmental conditions.

MATERIALS AND METHODS

Plant Material and Plant Transformation

Arabidopsis (*Arabidopsis thaliana*) Col-0 was used as the genetic background for all experiments. For the *soc1* mutation, *soc1-2* (Lee et al., 2000) and *soc1-6* (SALK_138131) T-DNA insertion lines were used (Alonso et al., 2003). Homozygous mutant plants were selected based on their late-flowering phenotype, and the presence of the T-DNA was confirmed by PCR on genomic DNA. For detection of the wild-type *SOC1* allele in the *soc1-2* and *soc1-6* mutants, the primer pairs G-20046 (5′-CTTTTGGTTTGAACTAATCTTTGTC-3′)/G-19924 (5′-ATATCACAAACCGTTTAGAAGCTTC-3′) and PDS606 (5′-ATCTCATGAAAGGAGGTTGC-3′)/PDS607 (5′-GTCACTTGTCTGCTTGTTGC-3′) were used, respectively. For the T-DNA insertion alleles, the primer pairs G-11003 (5′-GTTCACGTAGTGGGCCATC-3′)/G-19924 for the *soc1-2* mutant and lba1 (Alonso et al., 2003) and PDS607 for *soc1-6* were used. All generated constructs were transformed into Col-0 plants, making use of *Agrobacterium tumefaciens* strain GV3101 or ASE and the floral dip method (Clough and Bent, 1998). Transgenic plants were identified by selective germination on one-half-strength Murashige and Skoog (0.5 MS) medium supplemented with kanamycin (50 mg L^{-1}) or on soil watered with BASTA (0.1%).

Plasmid Constructions

A Gateway destination vector suitable for the expression of genes of interest fused to the coding region of the rat GR domain was obtained by removing the *AGL11* coding region from vector NOB221. For this purpose, the *Bam*HI and *Nco*I restriction enzymes were used. Subsequently, the digested vector was blunted, followed by introduction of the Gateway conversion cassette (Invitrogen) downstream of the *GR* coding region and upstream of the *CaMV35S* promoter. This complete expression cassette was cloned as an *Asc*I/*Pac*I fragment into the binary vector pGD121 (de Folter et al., 2006), resulting in the Gateway-compatible GR destination vector pARC146. The open reading frames from *SEP3* and *AG* (Immink et al., 2009) were cloned into pARC146 by LR reactions.

The bait constructs for the yeast one-hybrid assays were obtained by cloning the *SOC1* regulatory sequences as *Not*I/*Spe*I fragments into the vector pINT-HIS3NB (Meijer et al., 1998). Two fragments from the *SOC1* promoter were selected: one from −663 to +82 (Fig. 3A) and the other from −864 to −397. Fragments were amplified with the primers PDS497 (5′-AGACACGTCGCTACTTAACG-3′)/PDS499 (5′-TCTTCTCGTTGTAGTTATGG-3′) and PDS496 (5′-CGAAATAATTAGTTTGTGTGG-3′)/PDS498 (5′-ATATCTTTCCATCCCAACAG-3′), respectively. These two fragments have overlap in sequence, but this region does not contain putative consensus CArG box-binding sites. Together, these two promoter elements represent the upstream region of the −966 to +960 1-kb *SOC1* promoter that has been described by Hepworth et al. (2002). The obtained bait vectors containing these promoter fragments were designated pARC1046 (*pSOC1* −663 to +82) and pARC1047 (*pSOC1* −864 to −397; Fig. 3A). In addition, a bait plasmid was generated covering the *SOC1* 5′ UTR. This fragment was amplified with PDS2572 (5′-TTATCTTTCTCCAAGAAATAAAAT-3′)/PDS2573 (5′-CATGACGAAGAGATCTTACC-3′) and spans the genomic region from +1 to +409. This fragment was cloned into pINT-HIS3NB, resulting in the bait construct CZN2030 (*5′-UTR-SOC1* +1 to +409). All the above indicated constructs were controlled by restriction analyses and sequencing of the inserted fragment (DETT sequencing kit; Amersham).

The 8,186-bp genomic *SOC1* (At2g45660; TAIR 10, Chromosome 2: 18806523.0.18814708) rescue fragment, which includes an approximately 3.7-kb upstream sequence, exons, introns, UTR sequences, and an approximately 1.2-kb downstream sequence, was amplified by PCR from genomic DNA isolated from Col-0 using Phusion polymerase (New England Biolabs), primer G-27271 (5′-AAACTCGTATAATAAAACCATATAGTTAA-3′), and primer G-27272 (5′-ACCAACATTTTCCAAATGAAATAAAC-3′). The resulting PCR product was purified and cloned into the pCR8/GW/TOPO Gateway entry vector (Invitrogen) to create pDP29, which was confirmed by Sanger sequencing. Subsequently, the *SOC1* genomic fragment was recombined from pDP29 into a Gateway-compatible pGREEN-IIS binary destination vector (pFK387), which provides resistance to BASTA for selection in plants, resulting in pDP36 (*gSOC1*). For visualization of the SOC1 protein and to facilitate ChIP, *SOC1* was tagged with mGFP6-6xHIS. For this purpose, we amplified a genomic subfragment of *SOC1* ranging from exon 2, which contains a unique *Age*I restriction site, to the last coding triplet before the stop codon of *SOC1* using primer G-27342 (5′-GTTATCTGAGGCATACTAAG-3′) and primer G-27264 (5′-CTGTCGGCCGCAGAACCGGATCCAGATCCAGATCCCTTTCTTGAAG-3′), and the *SOC1* 3′ region, which contains a unique *Aat*II restriction site, starting with the stop codon using primer G-26333 (5′-CAAACACCACCACCACCACCACTGATCTCCACTCAACAA-3′) and primer G-27272. The sequence encoding mGFP6-6xHIS was amplified from the pMD107 plasmid (Curtis and Grossniklaus, 2003) using primer G-26331 (5′-GGTTCTGCGGCCGACAGTAAAGGAGAAGAAC-3′) and primer G-26332 (5′-TTGTTGAGTGGAGATCAGTGGTGGTGGTGGTGGTGTTTG-3′). Finally, the three fragments were combined in an overlapping fusion PCR employing primers G-27342 and G-27272. The resulting PCR product was cut with *Age*I and *Aat*II, cloned into the corresponding sites of pDP29, and verified by Sanger sequencing. Finally, the *SOC1:mGFP6* genomic fragment was recombined into pFK387 to create pDP37 (*gSOC1:GFP*). Then, a red fluorescence-based construct was generated as a reference marker for the imaging of the *gSOC1:GFP* lines. For this purpose, the *TagRFP* coding region (Merzlyak et al., 2007) was tagged with a nuclear localization signal-encoding sequence and placed under the control of the constitutive *BETA-6 TUBULIN* (*TUB6*) gene promoter (At5g12250) in a binary vector backbone.

Yeast One-Hybrid Assays

Integration of the bait vectors into the yeast genome from the strain PJ69-4 (mating type α; James et al., 1996) was performed as described before (Meijer et al., 2000). In order to determine the background levels of expression for the *HIS3* reporter gene, various colonies from the independent yeast integrations were suspended in 100 μL of Milli Q and spotted as 5-μL droplets onto a series of plates with selective synthetic dropout medium lacking His but supplemented with 0, 5, 10, 15, 20, 25, 30, 40, 50, or 60 mM 3-amino-1,2,4-triazole (3-AT). Plates were incubated at 20°C for 7 d and then scored for growth (activation of the *HIS3* reporter gene). For each bait construct, three independent colonies were selected that had low levels of background growth (growth up to 10 mM 3-AT maximum). Screening of binding by MADS box type II TF dimers was performed by mating. The available collection of type II dimers in strain PJ69-4 (mating type A; Immink et al., 2009) was grown overnight at 30°C in liquid synthetic dropout medium lacking Trp. At the same time, the yeast bait clones also were grown in liquid synthetic dropout medium lacking His. All possible dimer-bait combinations were made by spotting 5-μL droplets on top of each other in a grid of 96 spots on synthetic dropout agar plates containing all essential amino acids. After mating and growth for 1 night at 30°C, the yeast spots were transferred to synthetic dropout plates lacking Trp/His by a 96-pin replicator. These plates were grown over 2 nights at 30°C, and afterward, yeast spots were suspended on a 96-well plate with 100 μL of sterile Milli Q water in each well. Finally, these suspensions were spotted onto a series of synthetic dropout selection plates without Trp/His and supplemented with a range of 3-AT concentrations (10–60 mM). Dimer-DNA interaction events were scored after 7 d of incubation at 20°C. Each dimer-bait combination was screened at least two times in independent experiments.

Reporter and GR Induction Assays

Seedlings for the reporter assays were grown on plates with 0.5 MS medium (Duchefa Biochemie) in a growth chamber under LD conditions (16/8-h day/

night regime, 21°C). For GR induction, the medium was supplemented with DEX (Sigma-Aldrich) at a final concentration of 10 μM. Before germination, seeds were vapor-phase sterilized, followed by stratification at 4°C for 3 d. The GUS assay was performed on 10-d-old seedlings (LD conditions) or on plants grown for 3 weeks under SD conditions followed by 3 d in LD conditions. The GUS assays were performed based on the protocol described previously (de Folter et al., 2006). Plant material was incubated in the GUS staining solution for 16 h at 37°C.

SOC1 Loci Sequence Data

Putative orthologous genes of *SOC1* were selected by BLAST search of the Arabidopsis *SOC1* locus sequence (AT2G45660) against plant genomic sequences available on the Phytozome Web site (http://www.phytozome.net) and in the *Brassica* database (Cheng et al., 2011). Next, two filtering criteria were applied to identify true orthologs among the BLAST hits: (1) reciprocal best hit; and (2) the locus containing the hit has to have annotations for at least the first and last *SOC1* exons. As a result, *SOC1* orthologous genes were identified in the genome of seven species: Arabidopsis (TAIR 10, Chromosome 2:18807538-18811045), *Arabidopsis lyrata* (V1.0, scaffold_4:22217070-22221788), *Brassica rapa* (V1.1, A05:2530045-2533747), *Citrus sinensis* (V1.0, scaffold00001:1502952-1509395), *Citrus clementina* (V0.9, scaffold_3:991596-998038), *Cucumis sativus* (V1.0, scaffold02229:5073026-5076945), and *Mimulus guttatus* (V1.0, scaffold_27:797423-801044). Then, for each gene, the 3.0-kb sequence upstream of the first exon was taken as the promoter sequence.

Phylogenetic Analysis of the *SOC1* Promoter Sequence

The promoter sequences of *SOC1* from Arabidopsis and its orthologous genes were aligned using MUSCLE (Edgar, 2004), and maximum-likelihood phylogenetic trees were generated from the resulting alignments using fastDNAmL (Olsen et al., 1994). The DNA substitution model Hasegawa-Kishino-Yano (HKY85) was selected by modeltest (Posada and Crandall, 1998) using the Akaike informational criterion based on log-likelihood scores of the alignment. The training set for the mutation rates comprised sequences containing exon 1 of *SOC1* and flanking regions (±100 bp), using the known location of that exon in each of the seven species. Models for "fast" and "slow" regimes were learned by training the HKY85 model on the training set alignment using the regions with and without gaps, respectively. Subsequently, the models for "slow" and "fast" regimes were used to calculate the likelihood for each column of the multiple alignments. These likelihood values were employed to calculate the log-likelihood ratio under a fast versus a slow mutation regime. This ratio represents the relative likelihood that any given nucleotide site is subjected to a faster or slower mutation rate and is related to functional constraints imposed on each site (Boffelli et al., 2003). The corresponding likelihood ratio curves were used to describe the mutation profile of the Arabidopsis *SOC1* promoter sequence. The curve is smoothed by means of a 20% trimmed mean over the 50-base window centered at each aligned site.

ChIP, Library Preparation, and High-Throughput Sequencing

ChIP was performed in triplicate using 1 g of tissue enriched for transition apices collected at zeitgeber 4 from plants grown for 15 d under SD conditions, followed by a shift to long days for 3 consecutive days to synchronously induce flowering. DNA was precipitated using 2.5 μL of a polyclonal anti-GFP antibody (Abcam; no. 290) from *gSOC1:GFP*, *soc1-2*, and *gSOC1;soc1-2* plants, the latter of which serve as negative controls. Precipitated DNA was fragmented on a Covaris S2 machine (duty cycle, 20%; intensity, 5; cycles per burst, 200; cycle time, 2 min) and tested for the enrichment of presumed SOC1 targets such as *SEP3* and *SOC1* itself by qPCR, using the primers G-31798 (5′-TTTGAGGCAATGTCGTGAAG-3′) and G-31799 (5′-CCCTTCCCATTACGTCTTGA-3′) for *SEP3*, G-31800 (5′-ATGATGGACGCTTGAAACCT-3′) and G-31801 (5′-GACAGGCATTTCCATCCAAC-3′) for *SOC1*, and G-47 (5′-GGCTGTTGTCCTGGTATTATTTCTC-3′) and G-15952 (5′-GAGGACTAAGGCAATAGTACATGTT-3′) for *ARR7* (negative control). The qPCRs were performed using the Bio-Rad Real-Time PCR SYBR Green Mix. Libraries for high-throughput sequencing were prepared as described previously (Yant et al., 2010), and 40-bp single-end sequencing was performed on an Illumina GAIIx instrument following the manufacturer's instructions.

ChIP-seq Analyses

ChIP-seq peak calling was essentially performed as described (Moyroud et al., 2011), except that the filtering parameters were slightly modified as follows: potential peaks were discarded if their mean coverage for any control would exceed the median average control coverage plus a tolerance of 6 SD in all peak regions. A minimum normalized fold change of at least 2-fold between sample and control was required in at least one replicate, as well as a shift in peak location between forward and reverse strand of 10 bp or more.

Expression Analysis

Total RNA was isolated using Trizol (Ambion) from Col-0, *soc1-2*, and *35S::SOC1* plants grown in the same conditions and using the same tissue as in the ChIP experiment (15 d of SD conditions + 3 d of LD conditions). One microgram of total RNA was DNase I treated, and single-stranded complementary DNA was synthesized using oligo(dT) and the RevertAid first-strand complementary DNA synthesis kit (Fermentas). Quantitative real-time PCR was performed on an Opticon continuous fluorescence detection system (Bio-Rad [MJ Research Models]) using the Platinum SYBR Green qPCR Supermix-UDG (Invitrogen). Gene expression was calculated relative to β-tubulin using the ΔΔCt method (Livak and Schmittgen, 2001). Three biological and technical replicates were used for the quantification. Oligonucleotide primers used are as follows: for *β-TUB2*, N-0078 (5′-GAGCCTTACAACGCTACTCTGTCTGTC-3′) and N-0079 (5′-ACACCAGACATAGTAGCAGAAATCAAG-3′); for *SOC1*, G-0628 (5′-ATAGGAACATGCTCAATCGAGGAGCTG-3′) and G-0629 (5′-TTTCTTGAAGAACAAGGTAACCCAATG-3′); for *SVP*, G-20863 (5′-CAAGGACTTGACATTGAAGAGCTTCA-3′) and G-20864 (5′-CTGATCTCACTCATAATCTTGTCAC-3′); for *AGL18*, G-33582 (5′-ACCATTCCGACACTTCCTTG-3′) and G-33583 (5′-GAAGCCACTTGACTCCCAGA-3′); for *TEM2*, G-22652 (5′-GACTAGAGCGGCAGTTATATATTGAT-3′) and G-22653 (5′-CTTTCCACCGCAAACGGCCA-3′); for *AP2*, G-26366 (5′-TACACGTACTTCGCCGACAA-3′) and G-26367 (5′-GGTGTCGAACAAACCCAAAT-3′); for *SNZ*, G-0658 (5′-AGGGAGAAGGAGCCATGAAGTTTGGTG-3′) and G-0659 (5′-GTCTTCAGAGGTTTCATGGTTGCCATG-3′); for *SMZ*, G-4476 (5′-ATAAAATACAATGAGTTGGGAAAGGGA-3′) and G-4477 (5′-TGGTTGCCATGGGTAAAAATATCGATG-3′).

Confocal Imaging

Confocal laser scanning microscopy was performed to determine the expression and localization pattern of the SOC1 protein. The generated *gSOC1:GFP* lines in the Col-0 background were crossed with the *pTUB6::TagRFP* transgenic plants. From the progeny of this cross, a few lines were selected containing both constructs and showing the expected SOC1 expression pattern and constitutive expression of TagRFP. Seeds from these lines were sown, and the seedlings were grown for 21 d in SD conditions and 21°C to maintain the plants in the vegetative state. Subsequently, plants were transferred to LD conditions (21°C) to induce SOC1 expression in the SAM and, hence, flowering. Images from the SAM region were taken 0, 3, 5, and 7 d after the transfer to LD conditions. Imaging of the living plant tissue was performed with a Leica SPE DM5500 upright microscope as described previously (Urbanus et al., 2009).

Supplemental Data

The following materials are available in the online version of this article.

Supplemental Figure S1. qPCR to show the effect of SOC1 on the expression of seven loci bound by SOC1 according to the ChIP experiments.

Supplemental Figure S2. Maximum-likelihood phylogenetic tree of protein sequences encoded by *SOC1* orthologs found in flowering plants.

Supplemental Figure S3. Repression of *SOC1* by SEP3 and AG at the moment of floral transition.

Supplemental Table S1. SOC1 ChIP-seq sequence reads.

Supplemental Table S2. SOC1 ChIP-seq quality and position of peaks.

Supplemental Table S3. Summary of SOC1 ChIP-seq analyses and microarray expression studies.

Supplemental Table S4. Summary of yeast one-hybrid analyses.

ACKNOWLEDGMENTS

We thank Pieter Ouwerkerk for providing the pINT-HIS3NB plasmid and helpful advice on the yeast one-hybrid system; Iain Searle and George Coupland for seeds from the *pSOC1(1kb)*::*GUS* and *pSOC1(1kb)ΔCArG1*::*GUS* lines; Isabella Nougalli Tonaco for generating the *SEP3* and *AG* GR constructs and transgenic lines; Martin Kater for providing vector NOB221 containing a GR expression cassette; Frank Wellmer and Elliot Meyerowitz for providing seeds from the *AP1*:*GR* line; and Christa Lanz for assistance with Illumina sequencing.

Received June 26, 2012; accepted July 10, 2012; published July 12, 2012.

LITERATURE CITED

Adamczyk BJ, Lehti-Shiu MD, Fernandez DE (2007) The MADS domain factors AGL15 and AGL18 act redundantly as repressors of the floral transition in Arabidopsis. Plant J **50:** 1007–1019

Alon U (2007) Network motifs: theory and experimental approaches. Nat Rev Genet **8:** 450–461

Alonso JM, Stepanova AN, Leisse TJ, Kim CJ, Chen HM, Shinn P, Stevenson DK, Zimmerman J, Barajas P, Cheuk R, et al (2003) Genome-wide insertional mutagenesis of Arabidopsis thaliana. Science **301:** 653–657

Aukerman MJ, Sakai H (2003) Regulation of flowering time and floral organ identity by a microRNA and its *APETALA2*-like target genes. Plant Cell **15:** 2730–2741

Benlloch R, Kim MC, Sayou C, Thevenon E, Parcy F, Nilsson O (2011) Integrating long-day flowering signals: a LEAFY binding site is essential for proper photoperiodic activation of APETALA1. Plant J **67:** 1094–1102

Blazquez MA, Green R, Nilsson O, Sussman MR, Weigel D (1998) Gibberellins promote flowering of *Arabidopsis* by activating the LEAFY promoter. Plant Cell **10:** 791–800

Boffelli D, McAuliffe J, Ovcharenko D, Lewis KD, Ovcharenko I, Pachter L, Rubin EM (2003) Phylogenetic shadowing of primate sequences to find functional regions of the human genome. Science **299:** 1391–1394

Borner R, Kampmann G, Chandler J, Gleissner R, Wisman E, Apel K, Melzer S (2000) A MADS domain gene involved in the transition to flowering in Arabidopsis. Plant J **24:** 591–599

Castillejo C, Pelaz S (2008) The balance between CONSTANS and TEMPRANILLO activities determines FT expression to trigger flowering. Curr Biol **18:** 1338–1343

Cheng F, Liu S, Wu J, Fang L, Sun S, Liu B, Li P, Hua W, Wang X (2011) BRAD, the genetics and genomics database for Brassica plants. BMC Plant Biol **11:** 136

Clough SJ, Bent AF (1998) Floral dip: a simplified method for Agrobacterium-mediated transformation of Arabidopsis thaliana. Plant J **16:** 735–743

Corbesier L, Vincent C, Jang S, Fornara F, Fan Q, Searle I, Giakountis A, Farrona S, Gissot L, Turnbull C, et al (2007) FT protein movement contributes to long-distance signaling in floral induction of Arabidopsis. Science **316:** 1030–1033

Cubas P, Lauter N, Doebley J, Coen E (1999) The TCP domain: a motif found in proteins regulating plant growth and development. Plant J **18:** 215–222

Curtis MD, Grossniklaus U (2003) A Gateway cloning vector set for high-throughput functional analysis of genes in planta. Plant Physiol **133:** 462–469

de Folter S, Angenent GC (2006) trans meets cis in MADS science. Trends Plant Sci **11:** 224–231

de Folter S, Immink RGH, Kieffer M, Parenicová L, Henz SR, Weigel D, Busscher M, Kooiker M, Colombo L, Kater MM, et al (2005) Comprehensive interaction map of the *Arabidopsis* MADS box transcription factors. Plant Cell **17:** 1424–1433

de Folter S, Shchennikova AV, Franken J, Busscher M, Baskar R, Grossniklaus U, Angenent GC, Immink RGH (2006) A Bsister MADS-box gene involved in ovule and seed development in petunia and Arabidopsis. Plant J **47:** 934–946

Deng W, Ying H, Helliwell CA, Taylor JM, Peacock WJ, Dennis ES (2011) FLOWERING LOCUS C (FLC) regulates development pathways throughout the life cycle of Arabidopsis. Proc Natl Acad Sci USA **108:** 6680–6685

Dorca-Fornell C, Gregis V, Grandi V, Coupland G, Colombo L, Kater MM (2011) The Arabidopsis SOC1-like genes AGL42, AGL71 and AGL72 promote flowering in the shoot apical and axillary meristems. Plant J **67:** 1006–1017

Edgar RC (2004) MUSCLE: multiple sequence alignment with high accuracy and high throughput. Nucleic Acids Res **32:** 1792–1797

Franks SJ, Sim S, Weis AE (2007) Rapid evolution of flowering time by an annual plant in response to a climate fluctuation. Proc Natl Acad Sci USA **104:** 1278–1282

Gómez-Mena C, de Folter S, Costa MMR, Angenent GC, Sablowski R (2005) Transcriptional program controlled by the floral homeotic gene AGAMOUS during early organogenesis. Development **132:** 429–438

Goto K, Meyerowitz EM (1994) Function and regulation of the Arabidopsis floral homeotic gene PISTILLATA. Genes Dev **8:** 1548–1560

Gregis V, Sessa A, Colombo L, Kater MM (2008) AGAMOUS-LIKE24 and SHORT VEGETATIVE PHASE determine floral meristem identity in Arabidopsis. Plant J **56:** 891–902

Gregis V, Sessa A, Dorca-Fornell C, Kater MM (2009) The Arabidopsis floral meristem identity genes AP1, AGL24 and SVP directly repress class B and C floral homeotic genes. Plant J **60:** 626–637

Hartmann U, Höhmann S, Nettesheim K, Wisman E, Saedler H, Huijser P (2000) Molecular cloning of SVP: a negative regulator of the floral transition in Arabidopsis. Plant J **21:** 351–360

Hepworth SR, Valverde F, Ravenscroft D, Mouradov A, Coupland G (2002) Antagonistic regulation of flowering-time gene SOC1 by CONSTANS and FLC via separate promoter motifs. EMBO J **21:** 4327–4337

Honma T, Goto K (2001) Complexes of MADS-box proteins are sufficient to convert leaves into floral organs. Nature **409:** 525–529

Huang H, Tudor M, Su T, Zhang Y, Hu Y, Ma H (1996) DNA binding properties of two *Arabidopsis* MADS domain proteins: binding consensus and dimer formation. Plant Cell **8:** 81–94

Immink RG, Tonaco IA, de Folter S, Shchennikova A, van Dijk AD, Busscher-Lange J, Borst JW, Angenent GC (2009) SEPALLATA3: the 'glue' for MADS box transcription factor complex formation. Genome Biol **10:** R24

Ito T, Sakai H, Meyerowitz EM (2003) Whorl-specific expression of the SUPERMAN gene of Arabidopsis is mediated by cis elements in the transcribed region. Curr Biol **13:** 1524–1530

Izawa T (2007) Adaptation of flowering-time by natural and artificial selection in Arabidopsis and rice. J Exp Bot **58:** 3091–3097

Jack T, Fox GL, Meyerowitz EM (1994) Arabidopsis homeotic gene APETALA3 ectopic expression: transcriptional and posttranscriptional regulation determine floral organ identity. Cell **76:** 703–716

James P, Halladay J, Craig EA (1996) Genomic libraries and a host strain designed for highly efficient two-hybrid selection in yeast. Genetics **144:** 1425–1436

Kaufmann K, Muiño JM, Jauregui R, Airoldi CA, Smaczniak C, Krajewski P, Angenent GC (2009) Target genes of the MADS transcription factor SEPALLATA3: integration of developmental and hormonal pathways in the Arabidopsis flower. PLoS Biol **7:** e1000090

Kaufmann K, Pajoro A, Angenent GC (2010a) Regulation of transcription in plants: mechanisms controlling developmental switches. Nat Rev Genet **11:** 830–842

Kaufmann K, Wellmer F, Muiño JM, Ferrier T, Wuest SE, Kumar V, Serrano-Mislata A, Madueño F, Krajewski P, Meyerowitz EM, et al (2010b) Orchestration of floral initiation by APETALA1. Science **328:** 85–89

Kiełbasa SM, Vingron M (2008) Transcriptional autoregulatory loops are highly conserved in vertebrate evolution. PLoS ONE **3:** e3210

Lee H, Suh S-S, Park E, Cho E, Ahn JH, Kim S-G, Lee JS, Kwon YM, Lee I (2000) The AGAMOUS-LIKE 20 MADS domain protein integrates floral inductive pathways in Arabidopsis. Genes Dev **14:** 2366–2376

Lee J, Lee I (2010) Regulation and function of SOC1, a flowering pathway integrator. J Exp Bot **61:** 2247–2254

Lee J, Oh M, Park H, Lee I (2008) SOC1 translocated to the nucleus by interaction with AGL24 directly regulates leafy. Plant J **55:** 832–843

Lee JH, Yoo SJ, Park SH, Hwang I, Lee JS, Ahn JH (2007) Role of SVP in the control of flowering time by ambient temperature in Arabidopsis. Genes Dev **21:** 397–402

Li D, Liu C, Shen L, Wu Y, Chen H, Robertson M, Helliwell CA, Ito T, Meyerowitz E, Yu H (2008) A repressor complex governs the integration of flowering signals in Arabidopsis. Dev Cell **15:** 110–120

Liljegren SJ, Gustafson-Brown C, Pinyopich A, Ditta GS, Yanofsky MF (1999) Interactions among APETALA1, LEAFY, and TERMINAL FLOWER1 specify meristem fate. Plant Cell **11:** 1007–1018

Liu C, Chen H, Er HL, Soo HM, Kumar PP, Han JH, Liou YC, Yu H (2008) Direct interaction of AGL24 and SOC1 integrates flowering signals in Arabidopsis. Development **135:** 1481–1491

Liu C, Xi W, Shen L, Tan C, Yu H (2009) Regulation of floral patterning by flowering time genes. Dev Cell **16:** 711–722

Liu C, Zhou J, Bracha-Drori K, Yalovsky S, Ito T, Yu H (2007) Specification of Arabidopsis floral meristem identity by repression of flowering time genes. Development **134:** 1901–1910

Livak KJ, Schmittgen TD (2001) Analysis of Relative Gene Expression Data Using Real-Time Quantitative PCR and the $2^{-\Delta\Delta C_T}$ Method. Methods **25:** 402–408

Maere S, Heymans K, Kuiper M (2005) BiNGO: a Cytoscape plugin to assess overrepresentation of Gene Ontology categories in biological networks. Bioinformatics **21:** 3448–3449

Mandel MA, Yanofsky MF (1995) A gene triggering flower formation in Arabidopsis. Nature **377:** 522–524

Mathieu J, Warthmann N, Küttner F, Schmid M (2007) Export of FT protein from phloem companion cells is sufficient for floral induction in Arabidopsis. Curr Biol **17:** 1055–1060

Mathieu J, Yant LJ, Mürdter F, Küttner F, Schmid M (2009) Repression of flowering by the miR172 target SMZ. PLoS Biol **7:** e1000148

Meijer AH, Ouwerkerk PBF, Hoge JH (1998) Vectors for transcription factor cloning and target site identification by means of genetic selection in yeast. Yeast **14:** 1407–1415

Meijer AH, Schouten J, Ouwerkerk PBF, Hoge JHC (2000) Yeast as versatile tool in transcription factor research. *In* SR Gelvin, ed, Plant Molecular Biology Manual, Ed 2, Suppl IV. Kluwer Academic Publishers, Dordrecht, The Netherlands, pp E3: 1–28

Merzlyak EM, Goedhart J, Shcherbo D, Bulina ME, Shcheglov AS, Fradkov AF, Gaintzeva A, Lukyanov KA, Lukyanov S, Gadella TWJ, et al (2007) Bright monomeric red fluorescent protein with an extended fluorescence lifetime. Nat Methods **4:** 555–557

Michaels SD (2009) Flowering time regulation produces much fruit. Curr Opin Plant Biol **12:** 75–80

Michaels SD, Ditta G, Gustafson-Brown C, Pelaz S, Yanofsky M, Amasino RM (2003) AGL24 acts as a promoter of flowering in Arabidopsis and is positively regulated by vernalization. Plant J **33:** 867–874

Mizukami Y, Ma H (1992) Ectopic expression of the floral homeotic gene AGAMOUS in transgenic Arabidopsis plants alters floral organ identity. Cell **71:** 119–131

Moon J, Suh SS, Lee H, Choi KR, Hong CB, Paek NC, Kim SG, Lee I (2003) The SOC1 MADS-box gene integrates vernalization and gibberellin signals for flowering in Arabidopsis. Plant J **35:** 613–623

Moyroud E, Minguet EG, Ott F, Yant L, Posé D, Monniaux M, Blanchet S, Bastien O, Thévenon E, Weigel D, et al (2011) Prediction of regulatory interactions from genome sequences using a biophysical model for the *Arabidopsis* LEAFY transcription factor. Plant Cell **23:** 1293–1306

Nag A, King S, Jack T (2009) miR319a targeting of TCP4 is critical for petal growth and development in Arabidopsis. Proc Natl Acad Sci USA **106:** 22534–22539

Nilsson O, Lee I, Blázquez MA, Weigel D (1998) Flowering-time genes modulate the response to LEAFY activity. Genetics **150:** 403–410

Olsen GJ, Matsuda H, Hagstrom R, Overbeek R (1994) fastDNAmL: a tool for construction of phylogenetic trees of DNA sequences using maximum likelihood. Comput Appl Biosci **10:** 41–48

Palatnik JF, Allen E, Wu X, Schommer C, Schwab R, Carrington JC, Weigel D (2003) Control of leaf morphogenesis by microRNAs. Nature **425:** 257–263

Parcy F (2005) Flowering: a time for integration. Int J Dev Biol **49:** 585–593

Pastore JJ, Limpuangthip A, Yamaguchi N, Wu MF, Sang Y, Han SK, Malaspina L, Chavdaroff N, Yamaguchi A, Wagner D (2011) LATE MERISTEM IDENTITY2 acts together with LEAFY to activate APETALA1. Development **138:** 3189–3198

Posada D, Crandall KA (1998) MODELTEST: testing the model of DNA substitution. Bioinformatics **14:** 817–818

Riechmann JL, Krizek BA, Meyerowitz EM (1996) Dimerization specificity of Arabidopsis MADS domain homeotic proteins APETALA1, APETALA3, PISTILLATA, and AGAMOUS. Proc Natl Acad Sci USA **93:** 4793–4798

Rosenfeld N, Elowitz MB, Alon U (2002) Negative autoregulation speeds the response times of transcription networks. J Mol Biol **323:** 785–793

Sablowski RWM, Meyerowitz EM (1998) A homolog of NO APICAL MERISTEM is an immediate target of the floral homeotic genes APETALA3/PISTILLATA. Cell **92:** 93–103

Samach A, Onouchi H, Gold SE, Ditta GS, Schwarz-Sommer Z, Yanofsky MF, Coupland G (2000) Distinct roles of CONSTANS target genes in reproductive development of Arabidopsis. Science **288:** 1613–1616

Schmid M, Davison TS, Henz SR, Pape UJ, Demar M, Vingron M, Schölkopf B, Weigel D, Lohmann JU (2005) A gene expression map of Arabidopsis thaliana development. Nat Genet **37:** 501–506

Schommer C, Palatnik JF, Aggarwal P, Chételat A, Cubas P, Farmer EE, Nath U, Weigel D (2008) Control of jasmonate biosynthesis and senescence by miR319 targets. PLoS Biol **6:** e230

Schwarz-Sommer Z, Hue I, Huijser P, Flor PJ, Hansen R, Tetens F, Lönnig WE, Saedler H, Sommer H (1992) Characterization of the Antirrhinum floral homeotic MADS-box gene deficiens: evidence for DNA binding and autoregulation of its persistent expression throughout flower development. EMBO J **11:** 251–263

Seo E, Lee H, Jeon J, Park H, Kim J, Noh YS, Lee I (2009) Crosstalk between cold response and flowering in *Arabidopsis* is mediated through the flowering-time gene SOC1 and its upstream negative regulator FLC. Plant Cell **21:** 3185–3197

Sessions A, Nemhauser JL, McColl A, Roe JL, Feldmann KA, Zambryski PC (1997) ETTIN patterns the Arabidopsis floral meristem and reproductive organs. Development **124:** 4481–4491

Shore P, Sharrocks AD (1995) The MADS-box family of transcription factors. Eur J Biochem **229:** 1–13

Smaczniak C, Immink RGH, Muiño JM, Blanvillain R, Busscher M, Busscher-Lange J, Dinh QD, Liu S, Westphal AH, Boeren S, et al (2012) Characterization of MADS-domain transcription factor complexes in Arabidopsis flower development. Proc Natl Acad Sci USA **109:** 1560–1565

Song H-R, Song J-D, Cho J-N, Amasino RM, Noh B, Noh Y-S (2009) The RNA binding protein ELF9 directly reduces SUPPRESSOR OF OVEREXPRESSION OF CO1 transcript levels in *Arabidopsis*, possibly via nonsense-mediated mRNA decay. Plant Cell **21:** 1195–1211

Tao Z, Shen L, Liu C, Liu L, Yan Y, Yu H (2012) Genome-wide identification of SOC1 and SVP targets during the floral transition in Arabidopsis. Plant J **70:** 549–561

Treisman R (1986) Identification of a protein-binding site that mediates transcriptional response of the c-fos gene to serum factors. Cell **46:** 567–574

Tröbner W, Ramirez L, Motte P, Hue I, Huijser P, Lönnig WE, Saedler H, Sommer H, Schwarz-Sommer Z (1992) GLOBOSA: a homeotic gene which interacts with DEFICIENS in the control of Antirrhinum floral organogenesis. EMBO J **11:** 4693–4704

Turck F, Fornara F, Coupland G (2008) Regulation and identity of florigen: FLOWERING LOCUS T moves center stage. Annu Rev Plant Biol **59:** 573–594

Urbanus SL, de Folter S, Shchennikova AV, Kaufmann K, Immink RG, Angenent GC (2009) In planta localisation patterns of MADS domain proteins during floral development in Arabidopsis thaliana. BMC Plant Biol **9:** 5

van den Burg HA, Kini RK, Schuurink RC, Takken FLW (2010) *Arabidopsis* small ubiquitin-like modifier paralogs have distinct functions in development and defense. Plant Cell **22:** 1998–2016

Wang JW, Czech B, Weigel D (2009) miR156-regulated SPL transcription factors define an endogenous flowering pathway in Arabidopsis thaliana. Cell **138:** 738–749

Wang Y, Liu C, Yang D, Yu H, Liou Y-C (2010) Pin1At encoding a peptidyl-prolyl cis/trans isomerase regulates flowering time in Arabidopsis. Mol Cell **37:** 112–122

Wellmer F, Alves-Ferreira M, Dubois A, Riechmann JL, Meyerowitz EM (2006) Genome-wide analysis of gene expression during early Arabidopsis flower development. PLoS Genet **2:** e117

Winter CM, Austin RS, Blanvillain-Baufumé S, Reback MA, Monniaux M, Wu MF, Sang Y, Yamaguchi A, Yamaguchi N, Parker JE, et al (2011) LEAFY target genes reveal floral regulatory logic, cis motifs, and a link to biotic stimulus response. Dev Cell **20:** 430–443

Yant L, Mathieu J, Dinh TT, Ott F, Lanz C, Wollmann H, Chen X, Schmid M (2010) Orchestration of the floral transition and floral development in *Arabidopsis* by the bifunctional transcription factor APETALA2. Plant Cell **22:** 2156–2170

Yant L, Mathieu J, Schmid M (2009) Just say no: floral repressors help Arabidopsis bide the time. Curr Opin Plant Biol **12:** 580–586

Yoo SK, Chung KS, Kim J, Lee JH, Hong SM, Yoo SJ, Yoo SY, Lee JS, Ahn JH (2005) CONSTANS activates SUPPRESSOR OF OVEREXPRESSION OF CONSTANS 1 through FLOWERING LOCUS T to promote flowering in Arabidopsis. Plant Physiol **139:** 770–778

Zheng Y, Ren N, Wang H, Stromberg AJ, Perry SE (2009) Global identification of targets of the *Arabidopsis* MADS domain protein AGAMOUS-Like15. Plant Cell **21:** 2563–2577